Single Crystal Diffraction
- Charge Density Study

Yu Wang
Department of Chemistry
National Taiwan Univ.

Cheiron 2008
SPring-8, Oct.2, 2008

Outline:

Quick review on the single crystal diffraction

Model of non-spherical atom

Visulize the relationship between non-spherical atomic model and the chemical bonding by deformation density and partitioning of atom in molecule

Chemical system
normal covalent bond - organic molecule
M-L bond – coordination compounds
H-bond and intra / inter-molecular interactions

2

Structure factor (F_h) from a number of atoms (f_i)

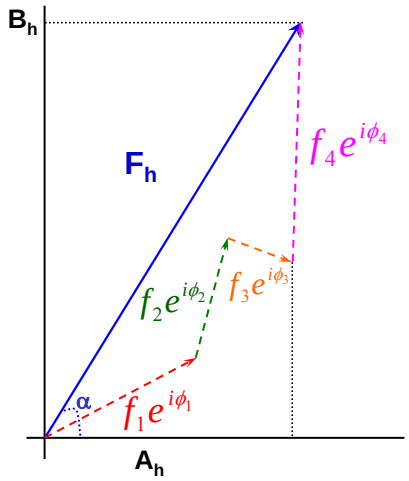

$$\phi_j = 2\pi(\sigma_h \cdot r_j)$$

$$F_h^{cal} = \sum_j f_j(h) e^{2\pi i \sigma_h \cdot r_j}$$

$$= |F| e^{i\alpha}$$

$$= |F| \cos\alpha - i|F| \sin\alpha$$

$$= A_h + iB_h$$

If centrosymmetric and no anomalous scatter:

B_h=0; α **=0 or** π

3

Structure factor F_h

Take the advantage of symmetry operators

$$F_h = \sum_j^{NA} g_j f_j \sum_i^{NE} \exp(2\pi i \bar{h} \cdot R_i \cdot \bar{x}_j)$$

$$= \sum_j^{NA} g_j f_i \left[2 \sum_i^{NE/2} \exp(2\pi i \bar{h} \cdot R_i \cdot \bar{x}_j) \right]$$ when $\bar{1}$ at (000)

g_j : atom multiplicity
R_i : sym. operator
$\bar{h}$: (h, k, l)
$\bar{x}_j$: (x_j, y_j, z_j)

NA : No. of atom types in an asymmetric unit

if $f_j = f_j^0 + \Delta f_j' + i\Delta f_j''$ **f : atomic amplitude**

then

$$A_h = \sum_j \left(f_j^0 + \Delta f_j'\right) \sum_i \cos 2\pi \left(h \cdot R_i \cdot x_j\right) - \sum_j \left(\Delta f_j''\right) \sum_i \sin 2\pi \left(h \cdot R_i \cdot x_j\right)$$

$$B_h = \sum_j \left(\Delta f_j''\right) \sum_i \cos 2\pi \left(h \cdot R_i \cdot x_j\right) + \sum_j \left(f_j^0 + \Delta f_j'\right) \sum_i \sin 2\pi \left(h \cdot R_i \cdot x_j\right)$$

4

Atomic amplitude with anomalous scattering

$$f_i = f_i^0\left(\frac{\sin\theta}{\lambda}\right) + \Delta f'(\lambda) + i\Delta f''(\lambda)$$

Nuclear thermal parameter: B;
thermal vibration T = B (sinθ/λ)²

with thermal vibration T as function of $(\sin\theta/\lambda)^2$

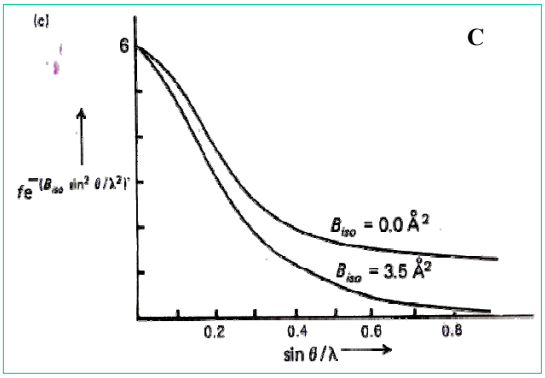

C atomic sphere (fixed atom at r_j)

B =0.0 at 0K
B = 3.5Å²

5

***f*⁰ for atoms from Z = 1 to 90**

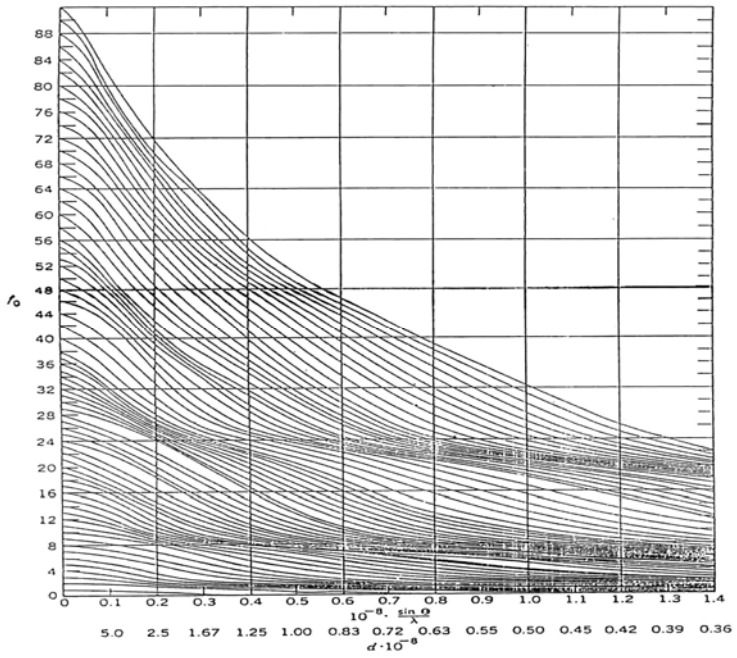

6

Considering nuclear thermal vibration

As a point scatterer, f_j

thermal vibration $\rightarrow$ electron density smearing
if isotropic $\leftrightarrow$ spherically symmetric

$$\rho \rightarrow \rho \exp\left[-B_{iso}\left(\frac{\sin^2\theta}{\lambda^2}\right)\right] = \rho \cdot T \qquad T < 1$$

f_j *is a function of* $\dfrac{\sin\theta}{\lambda}$

T *is a function of* $\dfrac{\sin^2\theta}{\lambda^2}$ T : *temperature factor*

$$B_{iso} = 8\pi^2 \langle u^2 \rangle$$

$\langle u^2 \rangle$ *mean square amplitude of vibration in* Å^2

7

Thermal ellipsoid

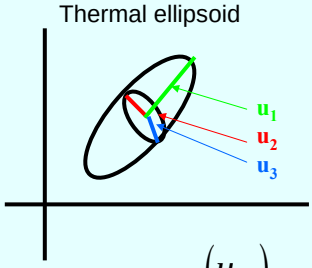

$$T = \exp\left(\sigma_h \cdot u_{ij} \cdot \sigma_k\right)$$
$$= \exp\left[-2\pi\left(u_{11}h^2a^{*2} + \cdots + 2u_{12}hka^*b^* + \cdots\right)\right]$$
$$= \exp\left[-\beta_{11}h^2 + \cdots + 2\beta_{12}hk + \cdots\right]$$
$$= \exp\left[-\frac{1}{4}\left(B_{11}h^2a^{*2} + \cdots + 2B_{12}hka^*b^* + \cdots\right)\right]$$

$\left(u_{ij}\right)$ diagonalize $\rightarrow$ $\begin{pmatrix} u_1 & 0 & 0 \\ 0 & u_2 & 0 \\ 0 & 0 & u_3 \end{pmatrix}$

eigen value $\leftrightarrow$ eigen function (three principle axes of the ellipsoid)

u_1 $\sum_i C_i^1 \tilde{a}_i$

u_2 $\sum_i C_i^2 \tilde{a}_i$

u_3 $\sum_i C_i^3 \tilde{a}_i$

8

Molecular structure with atomic thermal ellipsoids

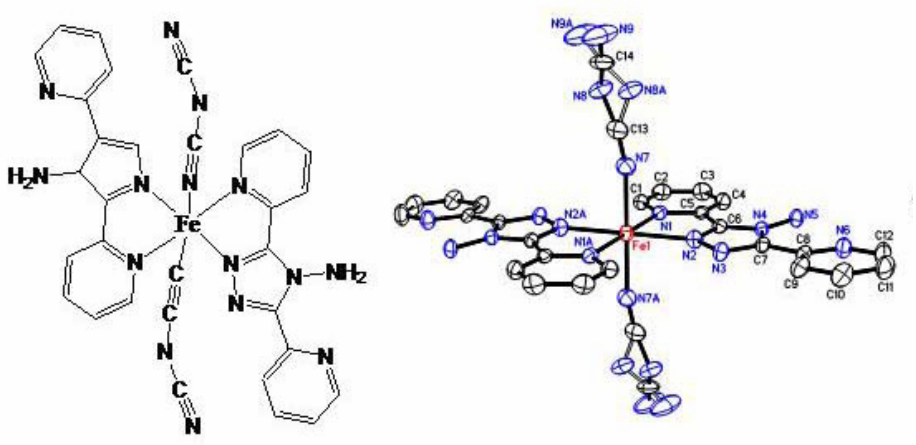

Relationship between F_{hkl} & ρ_{uvw}

Atomic scattering

$$df_i = \frac{1}{e}\rho(r)e^{2\pi\sigma_h r}dv \Rightarrow f_i = \frac{1}{e}\int \rho(r)e^{2\pi i\sigma_h r}dv$$

Crystal scattering general form with continuous ρ (u,v,w)

$$F_{\tilde{h}} = \int_v \rho(uvw)e^{2\pi i\tilde{\sigma}_h\cdot\tilde{u}}dv$$

$$F_{hkl} = \int_v \rho(uvw)\exp 2\pi i[hu+kv+lw]dv$$

$$F_{\tilde{h}} \xleftrightarrow{FT} \rho(uvw)$$

Corresponds to the intensity of h,k,l refln. reciprocal space

corresponds to the electron density at u,v,w position direction space

$$\rho(uvw) = \frac{1}{V}\sum_{-\infty}^{\infty}{}_{h,k,l}F_{h,k,l}e^{-2\pi i(hu+kv+lw)}$$

Fourier Transform

Between Direct Space ρ(x, y, z) and Reciprocal Space F(h, k, l)

$$\rho(\tilde{u}) = \sum\sum\sum C e^{-2\pi i(\tilde{h}\cdot\tilde{u})}$$

C: Fourier coefficient

C:

$\left(\lvert F^{obs}\rvert e^{-i\alpha_{F_c}}\right)/V$	$\rho(\tilde{u})$ **obs density (experiment)**
$F^{cal}_{\tilde{h}}/V$	**Calc density (model)**
$\frac{1}{V}\left(\lvert F^{obs}_{\tilde{h}}\rvert - \lvert F^{cal}_{\tilde{h}}\rvert\right)e^{i\alpha_{F_c}}$	**Difference density**
$\frac{1}{V}(E_{hk\ell})$	**E-map normalized density**
$F^2_{\tilde{h}}/V^2$	**Patterson density**

So far we have been modeling the structure as the sum of spherical atoms accompanied by their iso- or aniso thermal ellipsoids.

Can we obtain more information out of diffraction data in addition to the structure?

Can we see the bonding effect from the single crystal diffraction data?

XRD: *h,k,l*, I(*h,k,l*), σ(I)

⇓

***h,k,l*, F(*h,k,l*), σ(F)**

⇓ **FT**

ρ (x,y,z) total electron density at (x,y,z)

Evidence of the non-sphericity of atom in molecule

Deformation density

$\Delta\rho = \rho_{\text{total electron}} - \rho_{\text{spherical atom}}$

Laplacian of total electron density

$$\nabla^2\rho(r) = \partial^2\rho(r)/\partial x^2 + \partial^2\rho(r)/\partial y^2 + \partial^2\rho(r)/\partial z^2$$

$\rho_{\text{total electron}}$ **obtained from XRD and MO calculation**

13

Deformation density, Δρ

$\rho_{\text{total electron}} - \rho_{\text{spherical atom}}$

EXP: single crystal XRD

Theory: HF; DFT

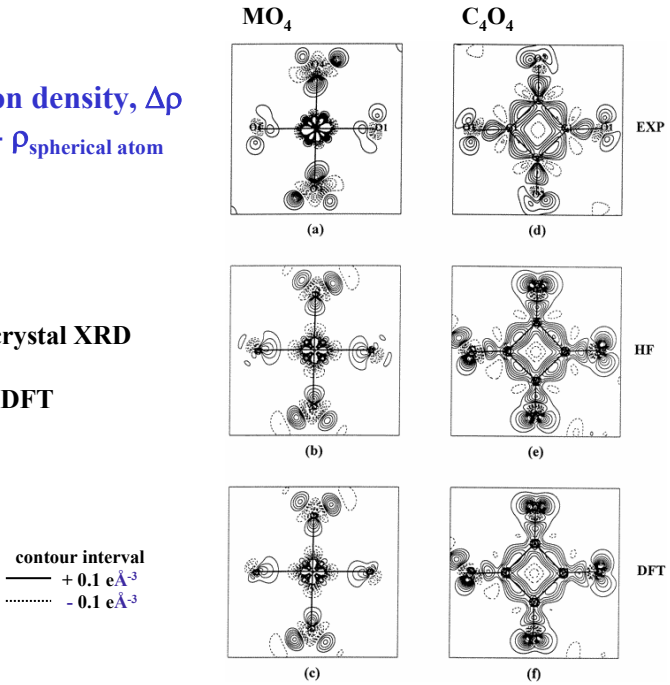

14

Models for non spherical atom

Hirshfeld's model

Σ R(r)cos$^n\theta_k$ **Isr. J. Chem 16, 226 (1977)**

$$\sum_{n=1}^{4}\sum_{4} N_n P_{jnk} r_j^{\,n} \exp(-\alpha r_j)\cos^n\theta_{jk}$$

Multipole model (Hansen & Coppens)

Σ R(r)Y$_{lm}(\theta,\phi)$ **AC A34, 909 (1978)**

$$\sum_{l=1}^{l_{\max}} \kappa'^3 R_l(\kappa' r)\sum_{m=0}^{l} P_{lm\pm} d_{lm\pm}(\theta,\phi)$$

15

Multipole Model

$$\rho_{at}(r) = P_c\rho_{core}(r) + P_v\kappa^3\rho_{valence}(\kappa r) + \sum_{l=1}^{l_{\max}} \kappa'^3 R_l(\kappa' r)\sum_{m=0}^{l} P_{lm\pm} d_{lm\pm}(\theta,\phi)$$

P_c : population coefficient of core electron density

P_v : population coefficient of valence electron

first two terms are spherical part of electron density of an atom

κ : scaling parameter → expansion or contraction of the valance shell

$R_l(\kappa' r)$: radial function → (1) *nodeless* (2) κ' scaling parameter

$d_{lm\pm}(\theta,\phi)$: angular part → (1) *real spherical harmonic* (2) $P_{lm\pm}$

third term is the part of non spherical part of electron density

16

Multipole Term--Angular Part

spherical harmonic function

$$Y_{lm}(\theta,\phi) = (-1)^m \left[\frac{(2l+1)}{4\pi} \frac{(l-|m|)!}{(l+|m|)!} \right]^{1/2} P_l^{|m|} \cos(\theta) \exp(im\phi)$$

$P_l^{|m|}$: Associated Legendre function

$$P_l^m(x) = (1-x^2)^{m/2} \left(\frac{d}{dx} \right)^{l+m} \frac{1}{2^l l!} (x^2-1)^l$$

Real spherical harmonic function

$$y_{l0} = Y_{l0} \qquad \text{for } m = 0$$

$$y_{lm+} = (-1)^m (Y_{lm} + Y_{l,-m})/2^{1/2} \qquad \text{for } m > 0$$

$$y_{lm-} = (-1)^m (Y_{lm} - Y_{l,-m})/(2^{1/2} i) \qquad \text{for } m > 0$$

17

$$y_{lm+}(\theta,\varphi) = N_{lm} P_l^m(\cos\theta) \cos m\phi \qquad 0 \leqq m \leqq l$$

$$y_{lm-}(\theta,\varphi) = N_{lm} P_l^m(\cos\theta) \sin m\phi \qquad 0 \leqq m \leqq l$$

Atomic wave function normalization $\int y_{lm\pm}^2 \, d\Omega = 1$

Ω : volume element in θ-ϕ space

$\int | d_{lm\pm} | \, d\Omega = 1$ for $l = 0$ $\qquad y_{lmp} = D_{lm} d_{lm\pm}$

$\int | d_{lm\pm} | \, d\Omega = 2$ for $l > 0$

For charge density function, the nonshperical functions ($l > 0$) represent a shift of density between regions of opposite signs. They have both positive and negative lobes which integrate to be equal but are with opposite number of electrons.

$$d_{lm+}(\theta,\varphi) = N'_{lm} P_l^m(\cos\theta) \cos m\phi$$

$$d_{lm-}(\theta,\varphi) = N'_{lm} P_l^m(\cos\theta) \sin m\phi$$

18

***l*=1, 2, 3, 4 as dipole, quadrupole, octapole and hexadecapole term**

l	symbol	Angular Function
0	00	1
1	11+	x
	11-	y
	10	z
2	20	$3z^2-1$
	21+	xz
	21-	yz
	22+	$(x^2-y^2)/2$
	22-	xy
3	30	$5z^3-3z$
	31+	$x[5z^2-1]$
	31-	$y[5z^2-1]$
	32+	$(x^2-y^2)z$
	32-	2xyz
	33+	x^3-3xy^2
	33-	$-y^3+3x^2y$

19

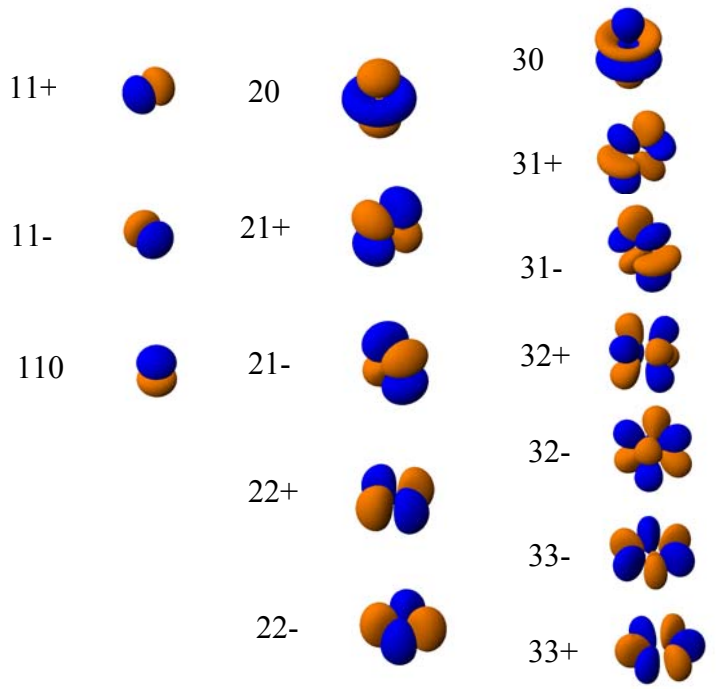

20

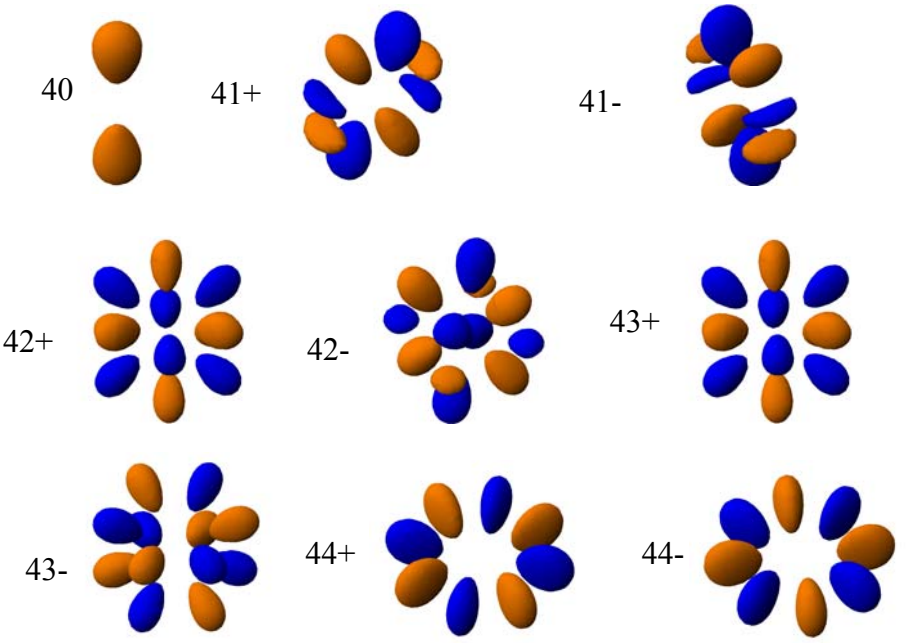

21

Multipole Term--Radial Part

Hydrogen 2s and 2p Slater-type orbital

$$R_{2s} = 2^{-1/2}\left(Z/a_0\right)^{3/2}\left(1 - Zr/2a_0\right)e^{-Zr/2a_0} \qquad R_{2p} = 24^{-1/2}\left(Z/a_0\right)^{5/2} re^{-Zr/2a_0}$$

Slater-type radial functions :(r^l) * (polynomial r^{n-l-1})

Number of nodes : *n-l-1*

The radial node is omitted in density function description.
Thus, defined as

$$R_l(r) = \kappa'^3 \frac{\zeta^{n_l+3}}{(n_l+2)!}(\kappa' r)^{n_l} \exp(-\kappa'\zeta_l r)$$

κ': the expansion –contraction parameters of the deformation functions

$r_{max} = n_l / \kappa' \zeta$

22

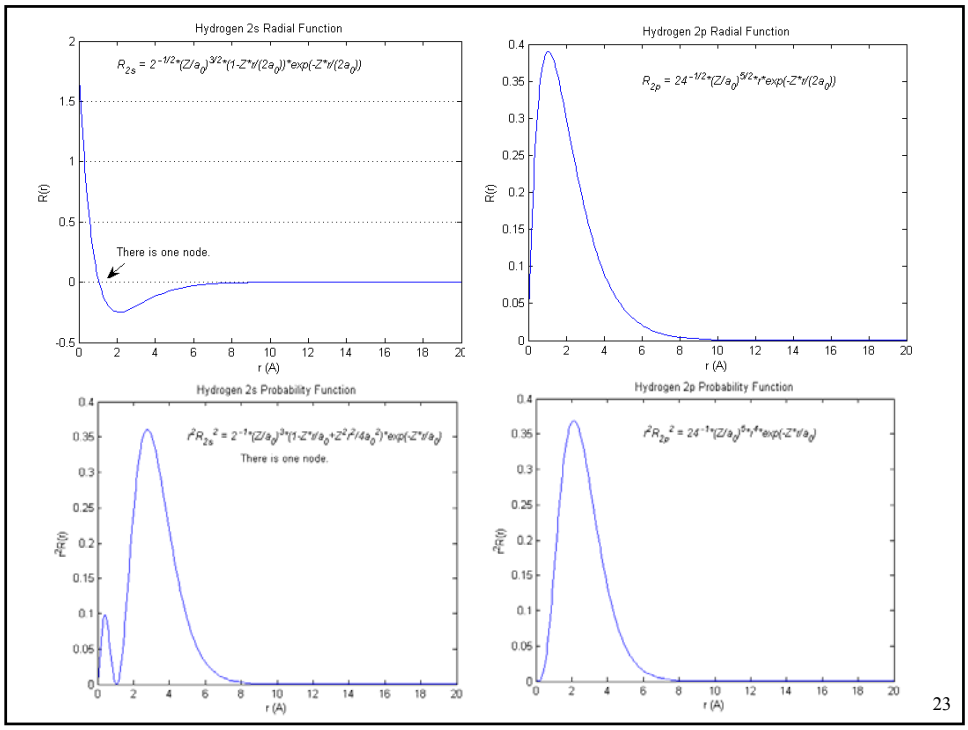

23

κ'=1,
ζ=3.176/0.529

dipole

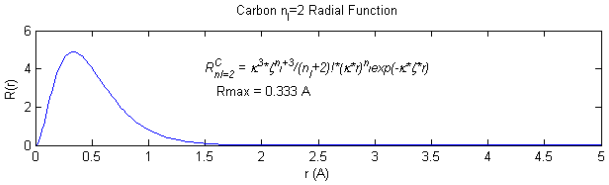

quadrupole

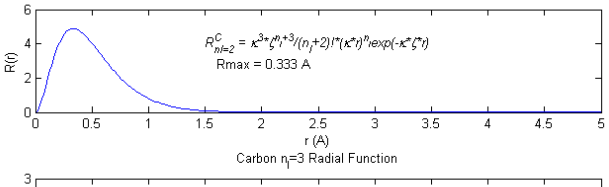

octapole

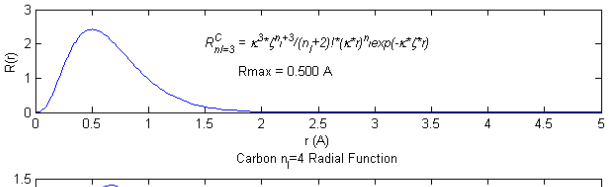

hexadecapole

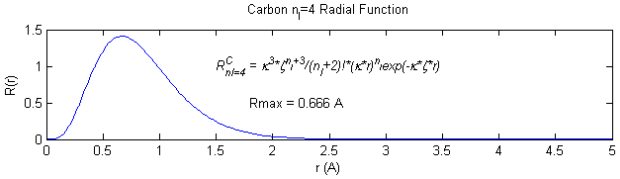

24

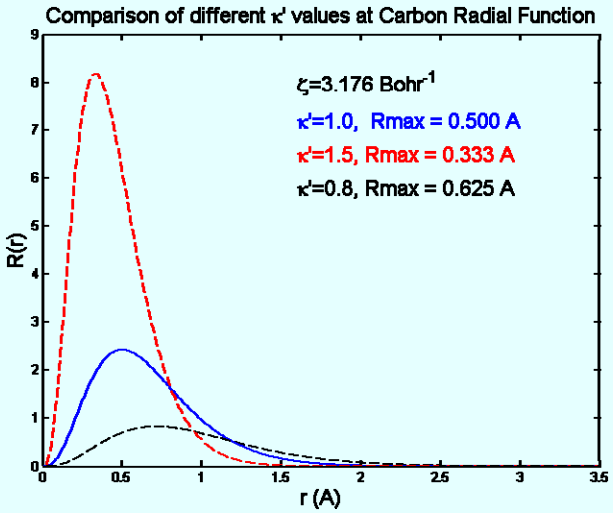

Recommended n_l value

	Dipole	Quadrupole	Octupole	Hexadecapole
l	1	2	3	4
1st-row atoms	2	2	3	4
2nd-row atoms	4	4	6	8

25

Scattering Factors of Aspherical Atom

Atomic form factor = FT[ρ]

$$f_j(\mathbf{S}) = \int \rho_j(r) \exp(2\pi\, \mathbf{S}\cdot\mathbf{r}) dr$$

$$\rho_{at}(r) = P_c \rho_{core}(r) + P_v \kappa^3 \rho_{valence}(\kappa r) + \sum_{l=1}^{l_{max}} \kappa'^3 R_l(\kappa' r) \sum_{m=0}^{l} P_{lm\pm} d_{lm\pm}(\theta,\phi)$$

$$f_j(\mathbf{S}) = P_{j.c} f_{j.core}(\mathbf{S}) + P_{j.v} f_{j.valence}(\mathbf{S}/\kappa) + \sum_{l=0}^{l_{max}} \sum_{m=0}^{l} \sum_{p} P_{lmp} f_{lmp}(\mathbf{S}/\kappa')$$

$$\mathbf{S} = \mathbf{H} = h\mathbf{a}^* + k\mathbf{b}^* + l\mathbf{c}^*$$

$$f_{lm\pm}(\mathbf{S}) = \int R_l(r) d_{lm\pm}(\theta,\phi) \exp(2\pi \mathbf{H}\cdot\mathbf{r}) d\mathbf{r}$$

26

Atomic scattering factors as f_{core} and $f_{valence}$

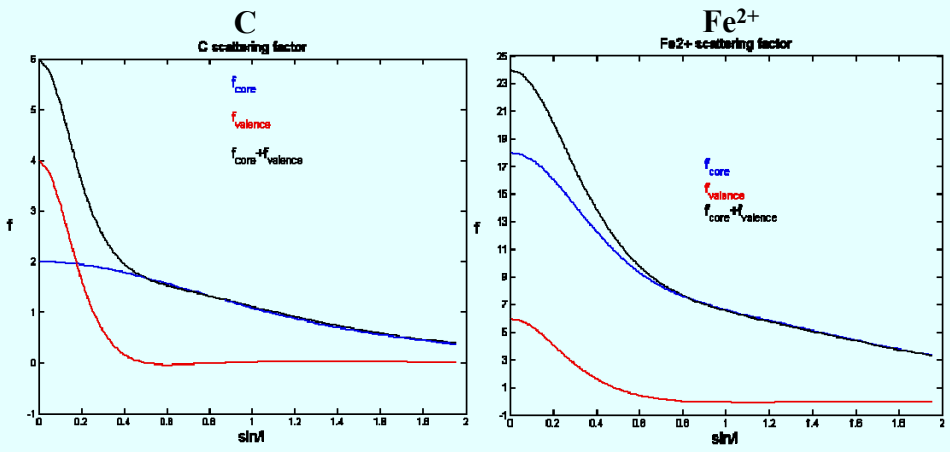

27

Summary

$$F(\mathbf{H}) = \sum_j \left[\left\{ \begin{array}{l} P_{j.c} f_{j.core}(H) + P_{j.v} f_{j.valence}(H/\kappa) \\ + 4\pi \sum_{l=1}^{l\max} \sum_{m=0}^{l} P_{lm\pm} i^l \left\langle j_l(S/\kappa') \right\rangle d_{lm\pm} \end{array} \right\} \exp(2\pi \mathbf{H}\cdot\mathbf{r}_j) T_j(\mathbf{H}) \right]$$

$\left\langle j_l \right\rangle = \int j_l(2\pi Sr) R_l(r) r^2 dr$ Fourier-Bessel transform

$T_j(\mathbf{H})$ temperature factor

κ : expansion-contraction in monopole density
κ': expansion –contraction in dipole, quadrupole, octapole and hexadecapole density

28

Visulize the relationship between
non-spherical atomic model
and
the chemical bonding

by
deformation density
and
partitioning of atom in molecule

Chemical system
normal covalent bond - organic molecule
M-L bond – coordination compounds
H-bond – intra or inter-molecular
interactions

29

$\Delta\rho_{def} = \rho_{mul} - \rho_{sph}$ $\sum_{l=0}^{l_{max}} \kappa'^3 R_l(\kappa' r) \sum_{m=0}^{l} P_{lm\pm} d_{lm\pm}(\theta,\phi)$ contours 0.1 eÅ^{-3}

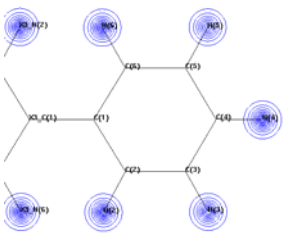

conv (without H)

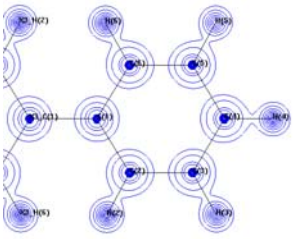

monopole ($l_{max} = 0$)

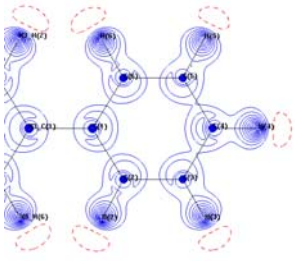

dipole ($l_{max} = 1$)

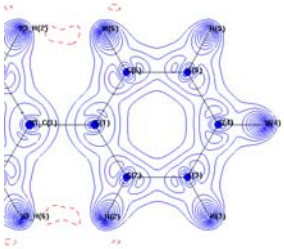

quadrupole ($l_{max} = 2$)

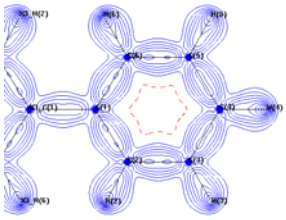

octapole ($l_{max} = 3$)

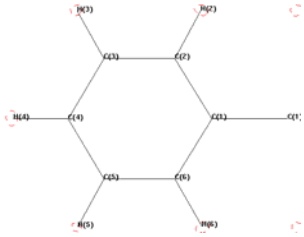

residual

30

Deformation Density, $\Delta\rho_{def}$

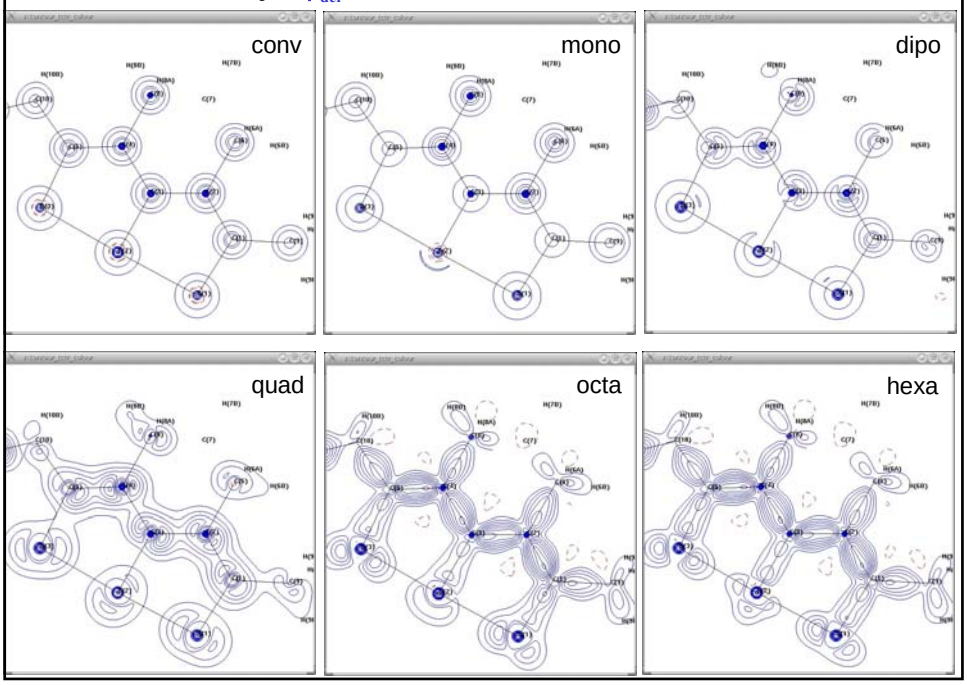

Residual Density from

Spherical model

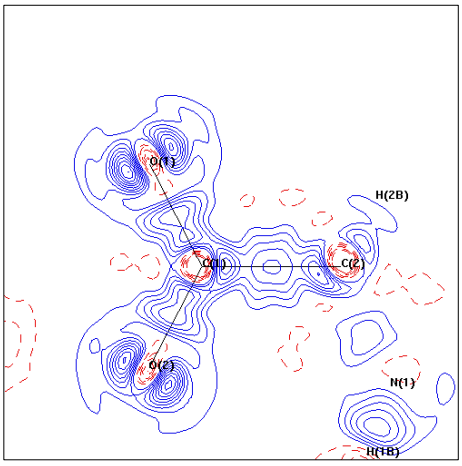

Multipolar model

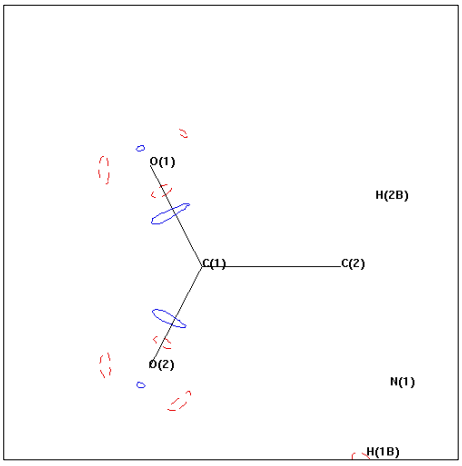

32

Atoms in Molecules (AIM)

Bader et al

first derivative $\nabla\rho$ — total electron density ρ — second derivative $\nabla^2\rho$

Gradient vector field

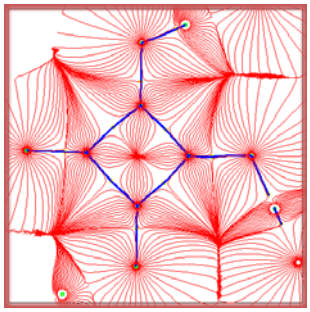

bond path

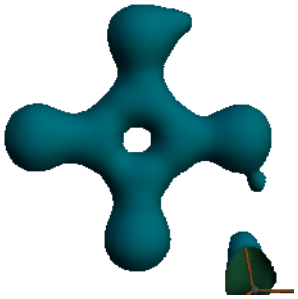

Laplacian

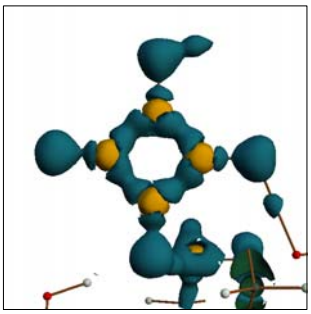

$\nabla^2\rho<0$ local concentration

$\nabla^2\rho>0$ local depletion

33

Critical Points

$$\nabla\rho = i\frac{d\rho}{dx} + j\frac{d\rho}{dy} + k\frac{d\rho}{dz} \rightarrow \begin{cases} = \vec{0} & (At\ critical\ \ points\ \ and\ \ at\ \ \infty) \\ generally \neq \vec{0} & (\ At\ \ all\ \ others\ \ points) \end{cases}$$

critical points are classified according to their **rank (ω)** and **signature (σ)**

(ω, σ)

(3, -3) : nuclear critical point (NCP)

(3, -1) : bond critical point (BCP)

(3, +1) : ring critical point (RCP)

(3, +3) : cage critical point (CCP)

34

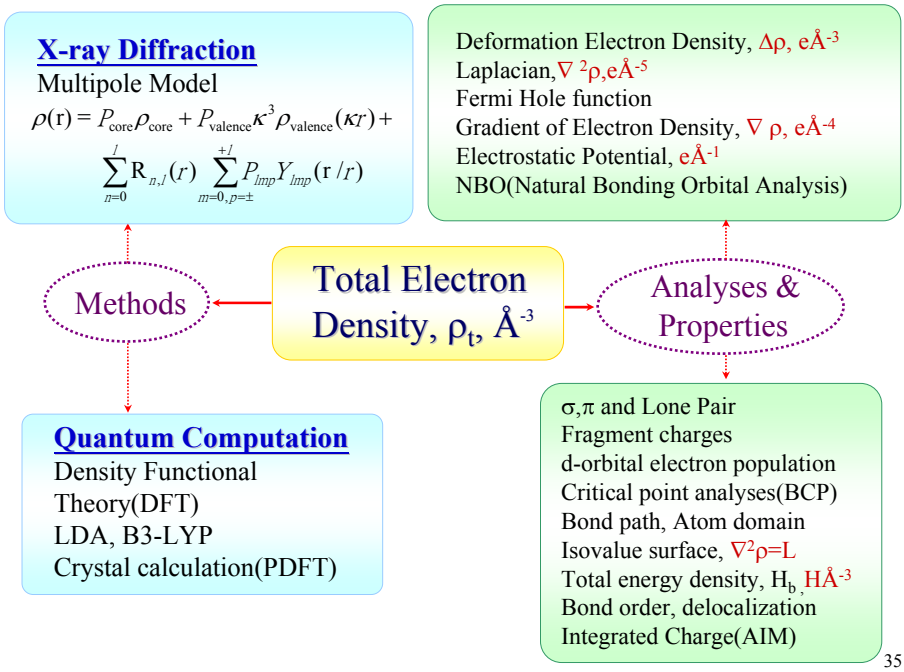

35

Chemical Bond

- **Covalent bond in organic molecule**
- **M-L coordinated bond**
- **M-L covalent bond**
- **Electronic configuration of M center**
- **H – bond and weak intermolecular interaction**

36

Covalent Bond in Ligand

Oxalic acid, $H_2C_2O_4$

Squarate, $C_4O_4^{2-}$

37

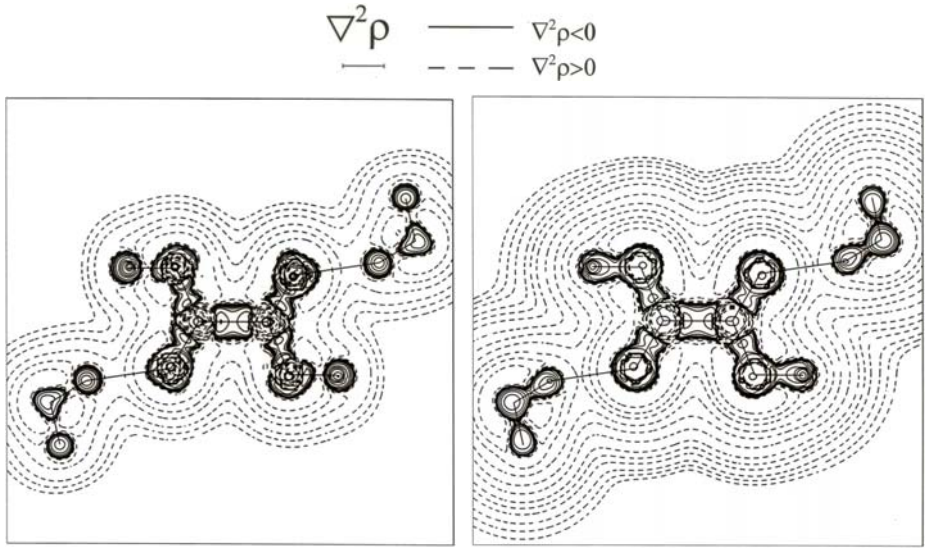

Expt. **DFT**

38

Properties at BCP of Oxalic Acid

a. Expt. b. DFT

Bond /BL (Å)		d1* (Å)	$\nabla^2\rho(r_c)$ $\lambda_1+\lambda_2+\lambda_3$ (eÅ^{-5})	$\rho(r_c)$ (eÅ^{-3})	H_b (HartreeÅ^{-3})
C-O Bond					
C1-O1	a	0.506	-26.16	2.51	
1.289(1)	b	0.422	-2.03	2.29	-3.698
C1-O2	a	0.484	-29.32	2.89	
1.223(1)	b	0.406	0.10	2.73	-4.691
C-C Bond					
C1-C1A	a	0.772	-16.42	1.99	
1.544(1)	b	0.772	-15.43	1.72	-1.410
Intermolecular hydrogen-bond					
O2-H3	a	1.201	4.15	0.12	
2.06(1)	b	1.213	4.03	0.19	-0.002

O2···O3 distance:2.830(1)

***distance from first atom to BCP**

39

Deformation density, $\Delta\rho$

Expt

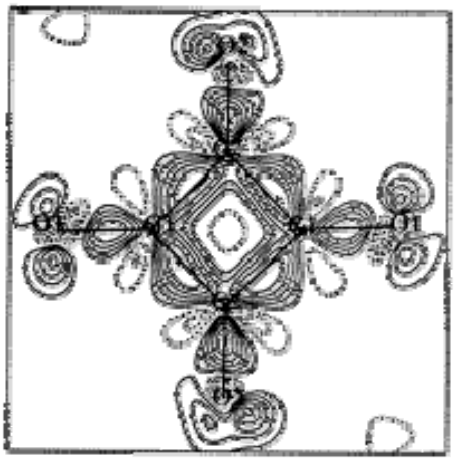

DFT

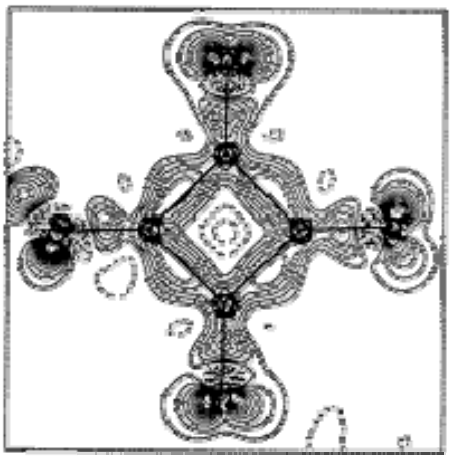

40

Laplacian, $\nabla^2\rho$, of C_4O_4 plane

Expt DFT

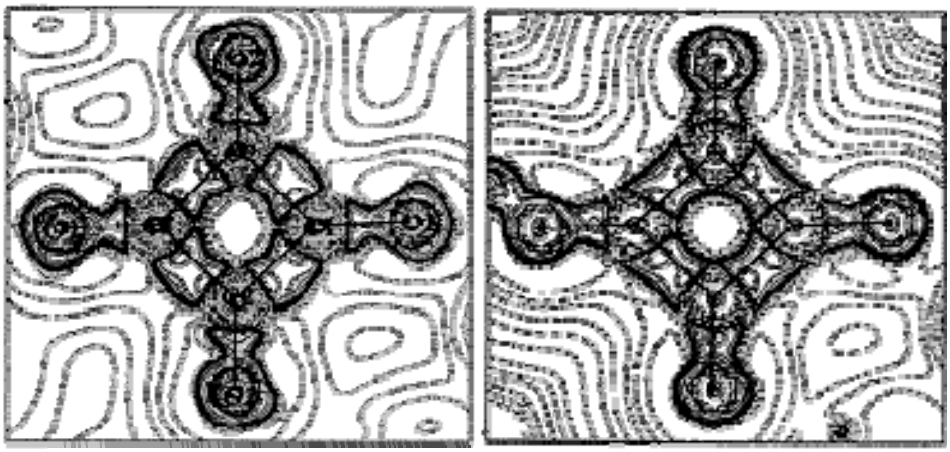

41

Bent bond of C_4O_4 plane

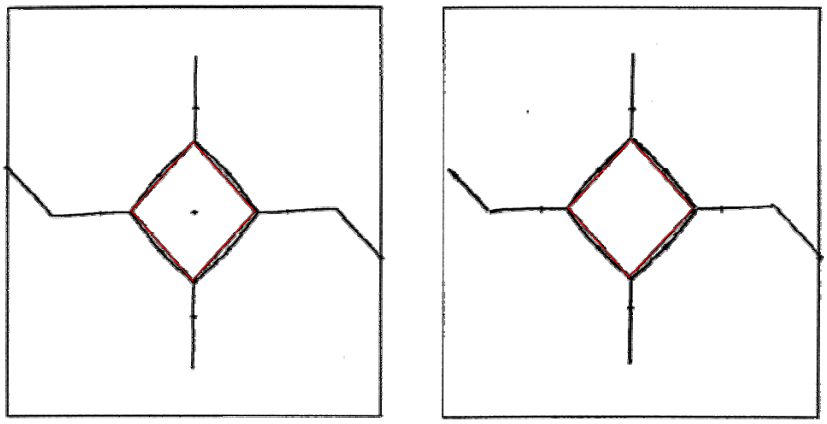

Expt DFT

Bond path (with BCP) and **interatomic axes** of the C_4O_4 plane of the Ni complex

42

Fermi hole functions from DFT

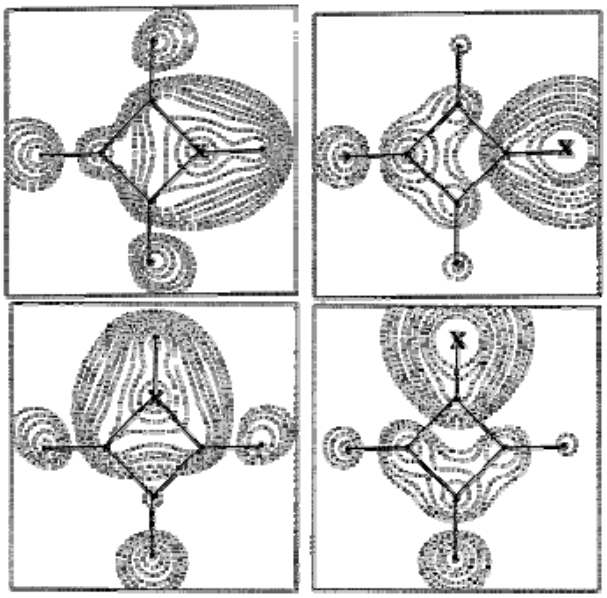

reference electron (x)

π delocalization of C_4O_4

43

$\nabla^2\rho$ of ClO_2 plane of ClO_4^-

Expt

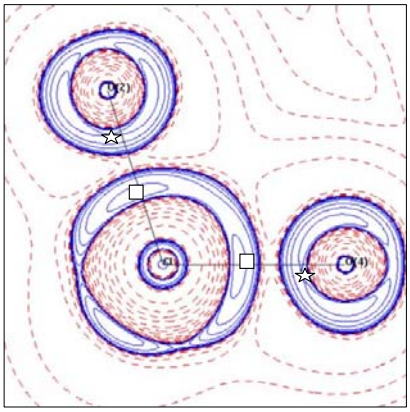

DFT

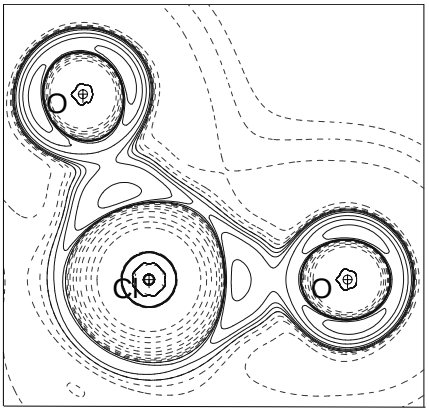

44

M-L coordinated Bond

4-coord.

$Ni(C_4N_4H_2)_2$ *J. Phy. Chem.*, **100,** 2934(1996); *J. Phy. Chem.*, **102,** 3726(1998).

$Ni(C_4N_4H_2)(S_2C_2(CF_3)_2)$

$Ni\ (S_2CN(C_2H_5)_2)_2$ *J. Phy. Chem. Solids*, **62,** 1613-1628(2001).

5-coord.

$Fe(NO)(S_2CNR_2)_2$

6-coord.

$[M(C_4O_4)(H_2O)_4]$ *J. Phys. Chem.*, **A103**, 156-165(1999)

$[Co^{II}(C_{12}H_{20}N_8)(H_2O)_2]\cdot 2ClO_4$ *Chem. Eur. J.*, **8**, 1821-1832(2002)

45

Structures

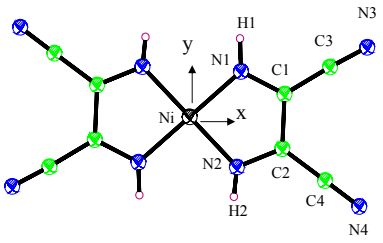

$Ni(C_4N_4H_2)_2$

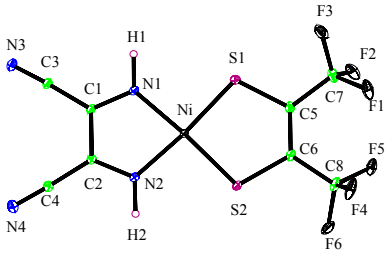

$Ni(C_4N_4H_2)(S_2C_2(CF_3)_2)$

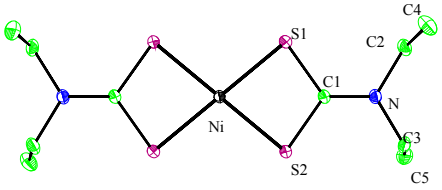

$Ni\ (S_2CN(C_2H_5)_2)_2$

46

$\nabla^2 \rho$ of $Ni(disn)_2$

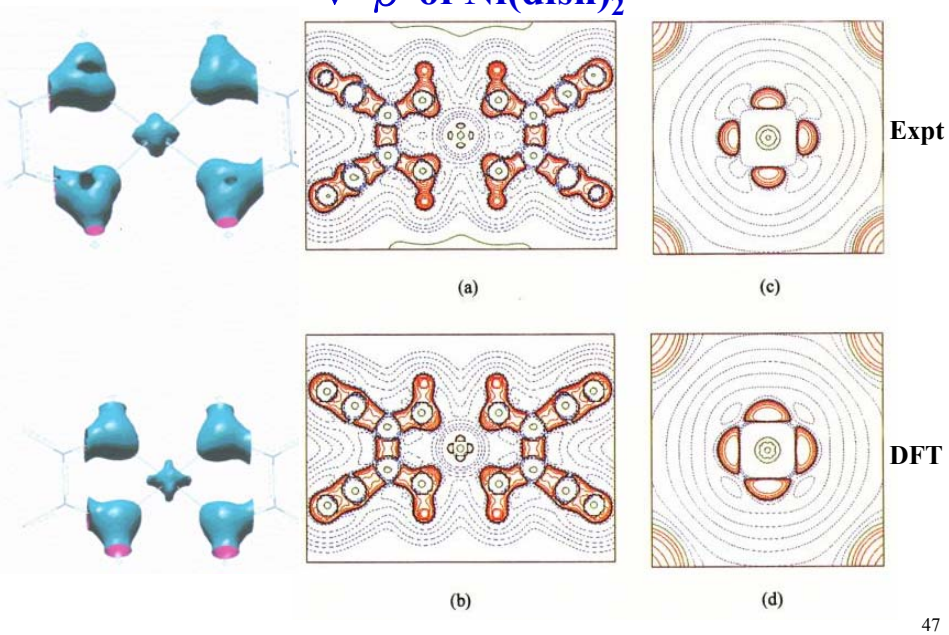

47

Laplacian Map around Ni

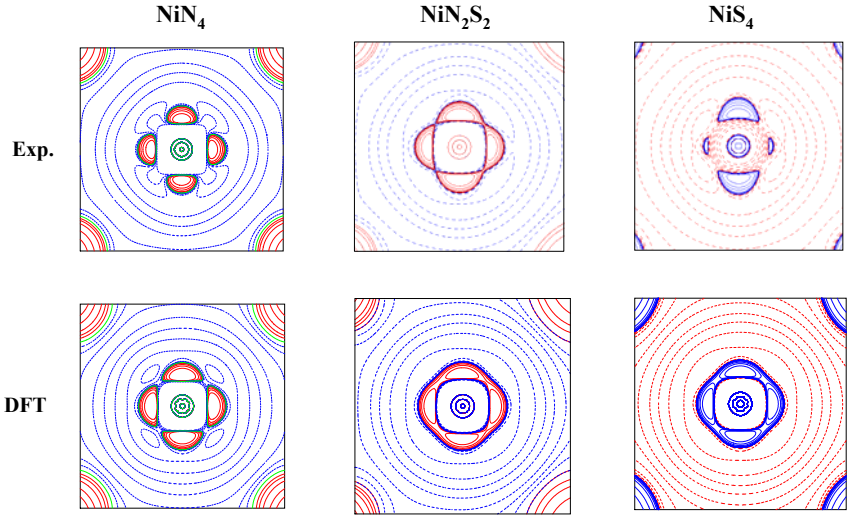

Laplacian maps of plane xy around Ni ion, contours are $\pm 2^i \times 10^j$, i = 1,2,3 and j = 0, 1,2

48

$Ni(disn)_2$

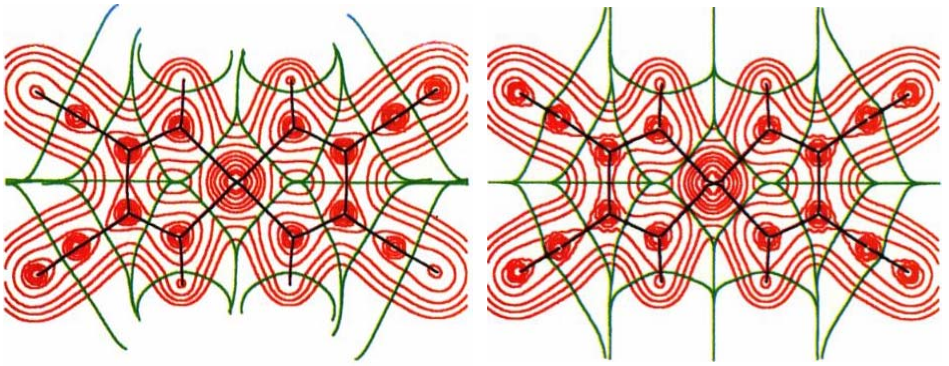

Experiment

Theory

Total electron density, bond path, **atom domain**

49

$Fe(NO)(S_2CNR_2)_2$

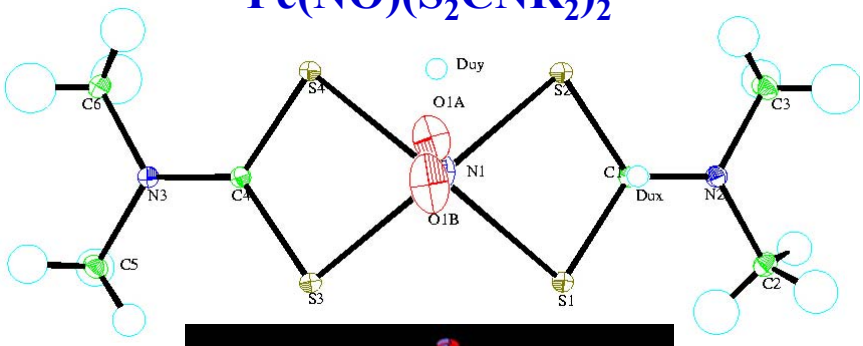

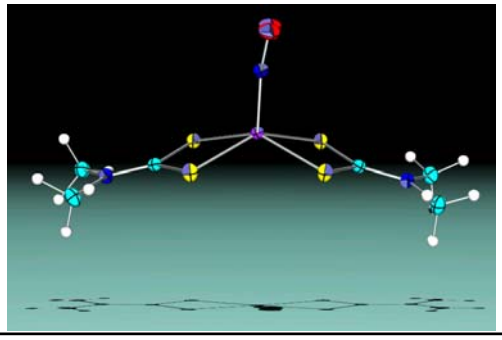

50

$\nabla^2 \rho$ at Fe-C1-S2 plane

Expt.

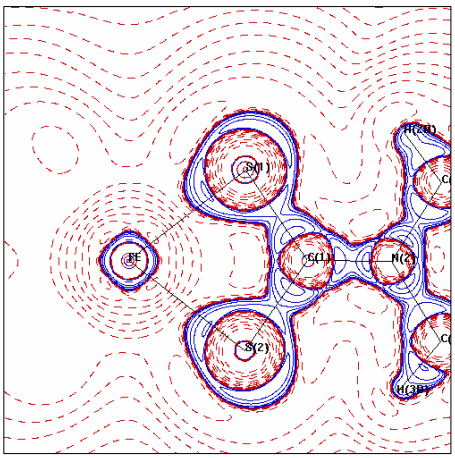

DFT/UB3LYP

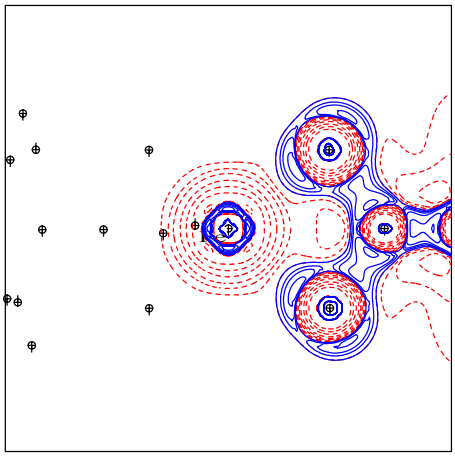

51

Properties of Selected Bond Critical point

1st line Multipole refinement 2nd line UB3LYP

Bond /Bond Length	d1 (Å)	ρ (r_c)	$\nabla^2 \rho$ (r_c)	H_b
FE -S(1)	1.053	0.508	3.756	-.172
/2.3138(1)	1.044	0.479	4.371	-.134
FE -S(2)	1.054	0.525	3.913	-.183
/2.2957(1)	1.036	0.496	4.625	-.142
FE -N(1)	0.869	1.340	23.259	-.765
/1.6907(4)	0.864	1.139	26.961	-.370
S(1)-C(1)	0.859	1.368	-4.237	
/1.7313(4)	0.758	1.379	-9.595	
S(2)-C(1)	0.855	1.373	-4.221	
/1.7272(4)	0.745	1.388	-9.528	
N(2)-C(1)	0.862	2.316	-22.129	
/1.3193	0.869	2.338	-18.661	
O(1a)-N(1)	0.859	4.441	-28.870	-10.30
/1.182(2)	0.521	3.664	-37.429	-7.87
Fe-S[a]		0.534	4.534	-.176
N-O[b]		4.006	-49.08	-7.87

a. Angew Chem. Int'l Ed..,**2000**,39, 3810.
b. R. F. W. Bader, Atoms in Molecules: A Quantum Theory, **1990**, Clarendon Press, Oxford.

Net Charge & Fragment Charge

Atom	DFT-NBO	DFT-Mulliken	DFT-AIM	Exp.-AIM
Fe	0.33	0.72	1.06	0.82
N1	0.10	-0.03	0.03	-0.15
O1	-0.21	-0.25	-0.40	-0.23
S_2CNEt_2	-0.11	-0.22	-0.35	-0.28
S_2CNEt_2	-0.10	-0.22	-0.33	-0.24

52

$[M(C_4O_4)(H_2O)_4]$; M=Fe, Co, Ni, Zn

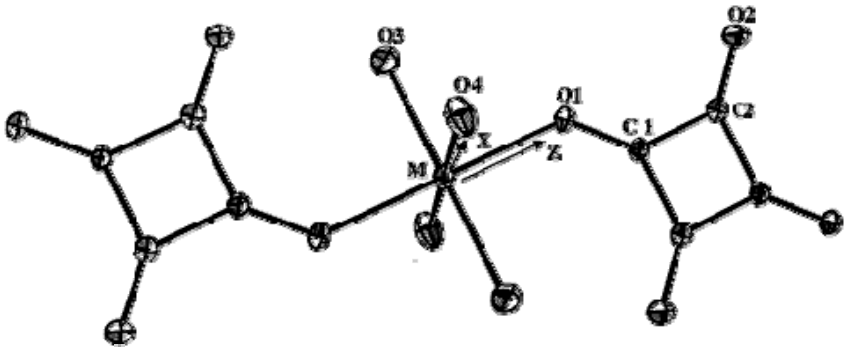

Molecular drawing with 50% probability in thermal ellipsoids at 120 K and choice of local Cartesian axis of metal centers.

53

Atom domain and total electron density

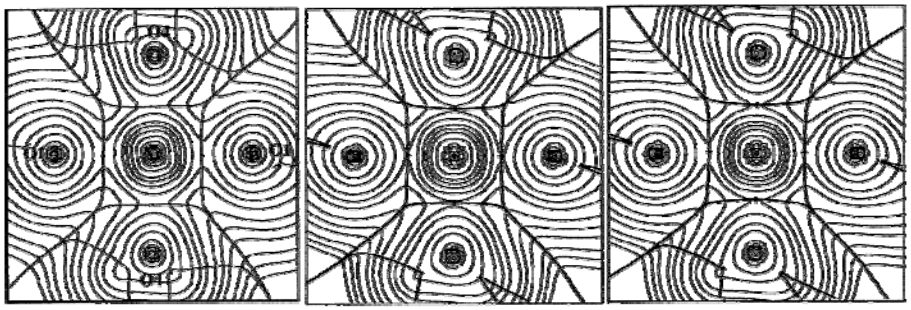

(a) Expt **(b) HF** **(c) DFT**

for the Ni center at the projection of the O1-Ni-O4 plane: (a) experiment; (b) HF; (c) DFT. contours of electron density are in steps of 2^m10^n e Å^{-3} (m = 1-3; n = -3 to +3).

54

$\nabla^2\rho$ of MO_4 plane

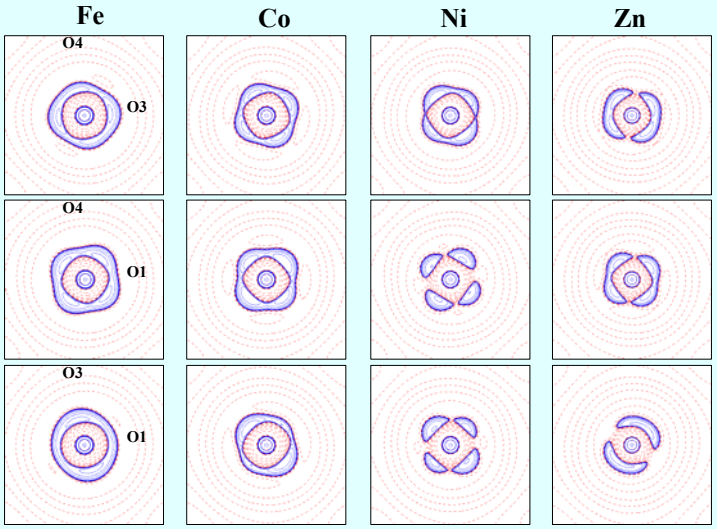

AIM	Fe	Co	Ni	Zn
Charge (e)	1.16	1.09	1.26	1.67
Volume (Å^3)	10.44	11.26	10.10	8.58

55

d-Orbital Populations of $M(C_4O_4)(H_2O)_4$

M	Fe	Co	Ni	Ni HF	Ni DFT	Zn
d_{z^2}	1.09(3)	0.98(4)	0.95(7)	1.09	1.22	1.36(7)
$d_{x^2-y^2}$	1.20(4)	1.11(5)	1.33(8)	1.06	1.15	1.64(8)
d_{xz}	1.43(5)	2.06(6)	2.02(9)	2.01	2.01	1.78(9)
d_{yz}	1.23(4)	1.22(6)	1.71(9)	1.98	2.02	1.55(9)
d_{xy}	1.10(4)	1.51(5)	1.84(8)	2.00	2.01	2.07(8)
Total	**6.05**	**6.88**	**7.89**	**8.14**	**8.41**	**8.40**

56

Fermi hole functions from DFT

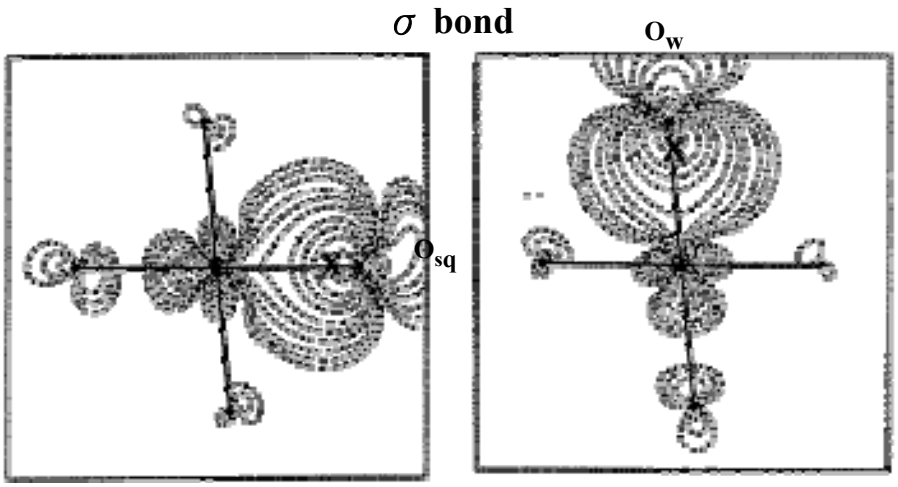

reference electron (**x**)

57

Molecular Structure of $[Co^{II}(C_{12}H_{20}N_8)(H_2O)_2]\cdot 2ClO_4$

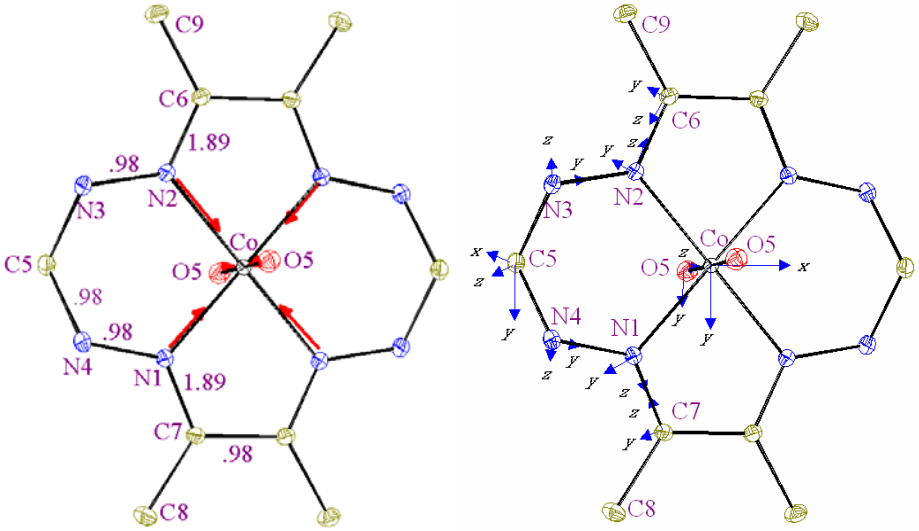

58

Total electron density, bond path, atom domain

Expt

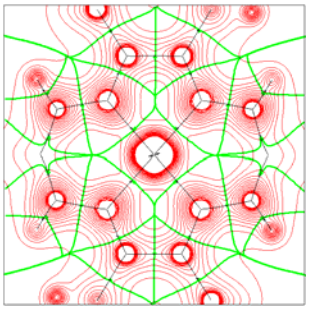

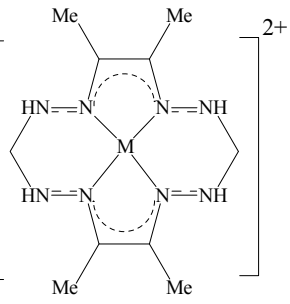

DFT

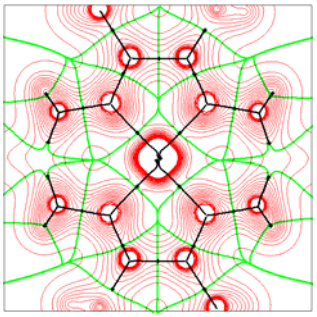

59

Gradient vector field of $[Co^{II}(C_{12}H_{20}N_8)(H_2O)_2]\cdot 2ClO_4$

Expt

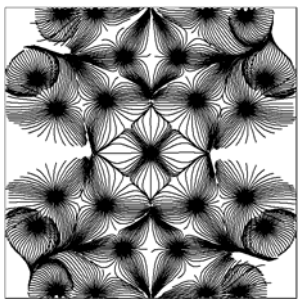

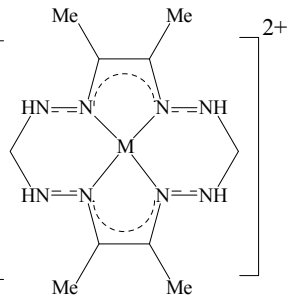

DFT

60

Fermi hole functions from DFT

σ bond

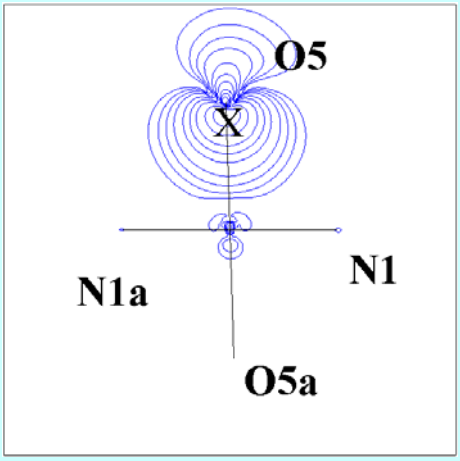

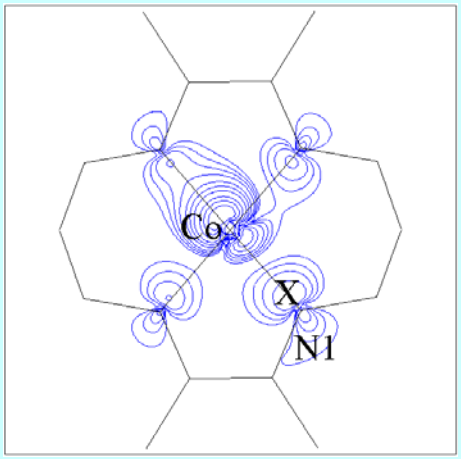

61

Topological Properties Associated with Bond Critical Points of M-L bond.

1st line: from experiment; 2nd line: from DFT

bond	compound	BL (Å)	d_1 (Å)	$\rho(r_c)$ (eÅ^{-3})	$\nabla^2\rho(r_c)$ (eÅ^{-5})	$H(r_c)$ (HatreeÅ^{-3})
M-S	$Co(S_2CNMe_2)_3$	2.2689(8)	1.07	0.49	4.62	-0.09
			1.01	0.51	4.96	-0.12
	$Ni(S_2CNEt_2)_2$	2.2011(7)	1.05	0.57	5.82	-0.11
			1.00	0.57	4.62	-0.20
	$Ni\,(C_4N_4H_2)\cdot(S_2C_2(CF_3)_2)$	2.1025(2)	0.97	0.73	7.10	-0.21
			0.96	0.73	5.10	-0.30
	$Fe(NO)(S_2CNEt_2)_2$	2.2963(1)	1.05	0.52	3.90	-0.18
			1.04	0.50	4.52	-0.14

62

Topological Properties Associated with Bond Critical Points of M-L bond

bond	compound	BL (Å)	d_1 (Å)	$\rho(r_c)$ (eÅ^{-3})	$\nabla^2\rho(r_c)$ (eÅ^{-5})	$H(r_c)$ (HatreeÅ^{-3})
M-N	$Ni(C_4N_4H_2)_2$	1.8325(7)	0.91	0.94	12.28	
			0.86	0.78	20.41	
	$Ni(C_4N_4H_2)\cdot(S_2C_2(CF_3)_2)$	1.8693(7)	0.93	0.82	12.18	-0.19
			0.90	0.77	14.38	-0.19
	$Co[(C_{12}H_{20}N_8)\cdot(H_2O)_2]\cdot 2ClO_4$	1.9026(7)	0.93	0.78	11.98	-0.26
			0.87	0.51	18.17	-0.05
	Cr(bpb)N	1.967(2)	0.99	0.72	11.69	
			0.97	0.70	9.80	-0.11
M-O	$Ni(C_4O_4)(H_2O)_4$	2.0381(7)	1.02	0.47	8.07	
			0.98	0.38	8.94	
	$Co(C_4O_4)(H_2O)_4$	2.0767(4)	1.03	0.46	7.36	
	$Fe(C_4O_4)(H_2O)_4$	2.1076(4)	1.05	0.40	7.09	
	$Co[(C_{12}H_{20}N_8)\cdot(H_2O)_2]\cdot 2ClO_4$	2.2854(9)	1.14	0.28	4.13	0.00
			1.08	0.13	4.14	-0.02

63

Molecular structure of four Cr-L multiple bond complexes

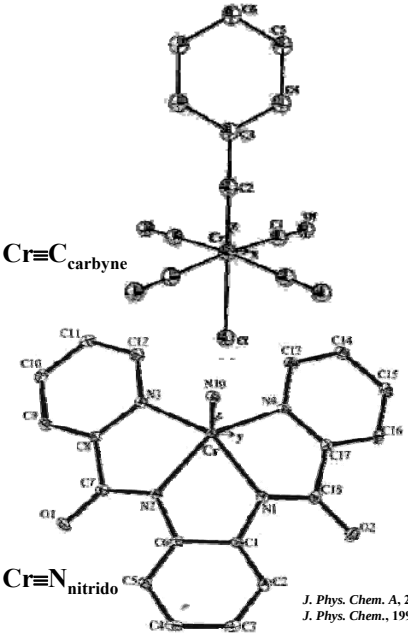

$Cr{\equiv}C_{carbyne}$

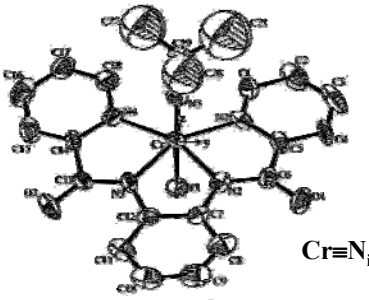

$Cr{\equiv}N_{imido}$

$Cr{\equiv}N_{nitrido}$

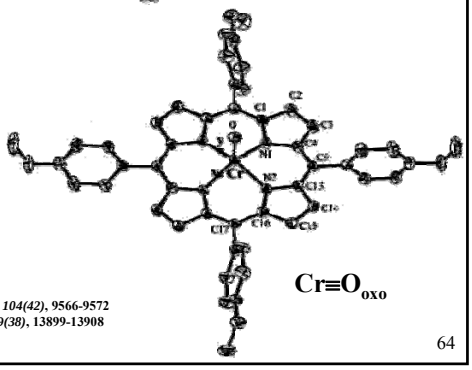

$Cr{\equiv}O_{oxo}$

J. Phys. Chem. A, 2000, *104(42)*, 9566-9572
J. Phys. Chem., 1995, *99(38)*, 13899-13908

64

Fermi Hole Distribution

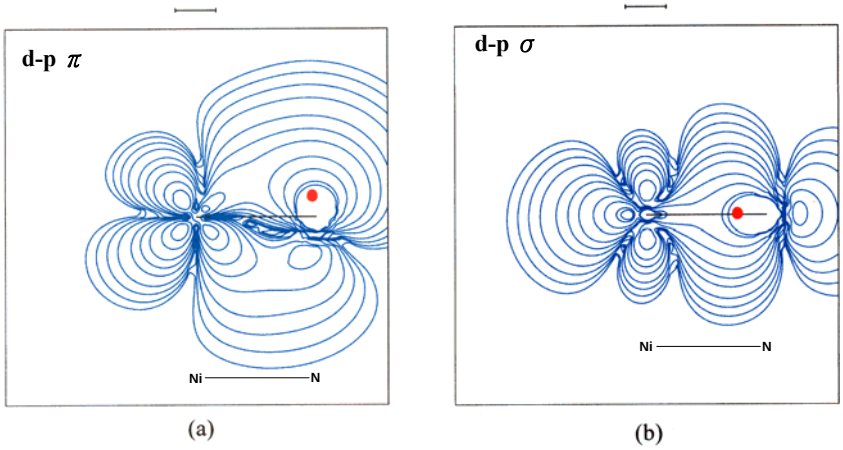

Fermi hole density with the reference electron (•) placed at 0.5 au away (a) and above (b) the $N_{nitrido}$ atom. The countours are in atomic unit with $-2^i \times 10^j$ (i = 0, 1, 2, 3; j = -3, -2, -1)

65

TABLE 2: Natural Bond Orbital Analysis of Cr−L Multiple Bonds

bond type	1. $[(CO)_4(Cl)Cr{\equiv}CPh]$ Cr−$C_{(carbyne)}$/1.725(4)[a] center	NHO	occ.	4. $[(TPP)Cr{\equiv}O]$ Cr−$O_{(oxo)}$/1.582(4)[a] center	NHO	occ.
σ	Cr	sd_{z^2} (35%)	1.921	Cr	sd_{z^2} (20%)	1.832
	$C_{carbyne}$	sp_z (65%)		O_{oxo}	sp_z (80%)	
π_1	Cr	d_{xz} (68%)	1.860	Cr	d_{xz} (27%)	1.952
	$C_{carbyne}$	p_x (32%)		O_{oxo}	p_x (73%)	
π_2	Cr	d_{yz} (69%)	1.810	Cr	d_{yz} (28%)	1.945
	$C_{carbyne}$	p_y (31%)		O_{oxo}	p_y (72%)	
bond type	2. [(bpb)Cr≡N] Cr−$N_{(nitrido)}$/1.555(2)[a] center	NHO	occ.	3. [(bpb)(Cl)Cr≡$N(CH_3)$] Cr−$N_{(imido)}$/1.63(1)[a] center	NHO	occ.
σ	Cr	sd_{z^2} (42%)	1.906	Cr	sd_{z^2} (24%)	1.956
	$N_{nitrido}$	sp_z (58%)		N_{imido}	sp_z (76%)	
π_1	Cr	d_{xz} (51%)	1.983	Cr	d_{xz} (39%)	1.726
	$N_{nitrido}$	p_x (49%)		N_{imido}	p_x (61%)	
π_2	Cr	d_{yz} (52%)	1.946	Cr	d_{yz} (40%)	1.944
	$N_{nitrido}$	p_y (48%)		N_{imido}	p_y (60%)	

[a] Bond length of Cr−L multiple bond (Å).

66

Topological properties at the BCP of the M–L multiple bonds

1st line from experiment, 2nd line from theory.

Bond	B. L.(Å)	d_1(Å)	$\rho(r_c)$(eÅ^{-3})	$\nabla^2\rho(r_c)$(eÅ^{-5})	$H(r_c)$	B.O.	BDE(kcal/mole)
Cr–$C_{carbyne}$	1.725	0.895 0.896	0.86 1.23	15.82 13.88	-0.618	2.44	115.2
W–$C_{carbyne}$	1.843	1.015	1.22	10.44	-0.699		155.0
Cr–$C_{carbene}$	1.999	0.998 0.973	0.68 0.67	9.41 9.02	-0.162		48.5
W–$C_{carbene}$	2.088	1.065	0.77	7.46	-0.272		75.0
Cr–$N_{nitrido}$	1.555	0.846 0.842	1.87 2.06	26.94 13.54	-1.728	2.72	
Mo–$N_{nitrido}$	1.728	0.959	2.49	10.14	-2.557		
W–$N_{nitrido}$	1.727	0.934	2.27	14.45	-2.286		
Cr–N_{imido}	1.630	0.847	1.48	23.92	-0.823	2.44	
Fe-$N_{nitrosyl}$	1.691	0.869 0.864	1.34 1.14	23.26 26.96	-0.765 -0.370		
Cr–O_{oxo}	1.582	0.815	1.83	23.54	-1.239	2.65	
Mo–O_{oxo}	1.755	0.932	2.15	21.07	-1.936		
W–O_{oxo}	1.732	0.914	2.02	25.48	-1.741		

67

Electronic configuration of M

Fe^{2+} $3d^6$

HS $t_{2g}^4 e_g^2$

LS $t_{2g}^6 e_g^0$

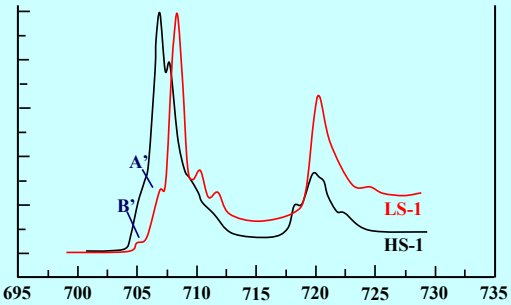

$L_{II,III}$-absorption edge of $Fe(Phen)_2(NCS)_2$

J. Am. Chem. Soc., 2000, *122(24)*, 5742-5747

68

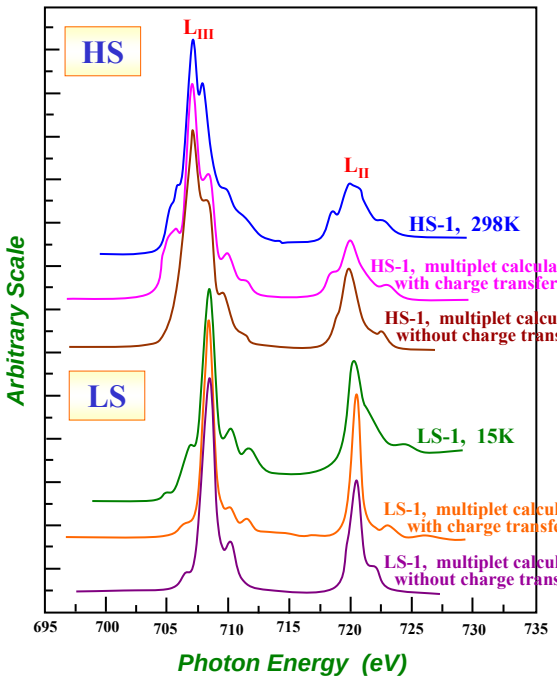

Multiplet Calculation

HS：10Dq = 0.91eV

LS：10Dq = 2.13eV

Experimental and Calculated $L_{II,III}$-absorption edge of $Fe(phen)_2(NCS)_2$ on 298K, 15K

JACS 2000, 122,5742-7

69

$\nabla^2\rho$ from Expt.

$Fe(abpt)_2(NCS)_2$

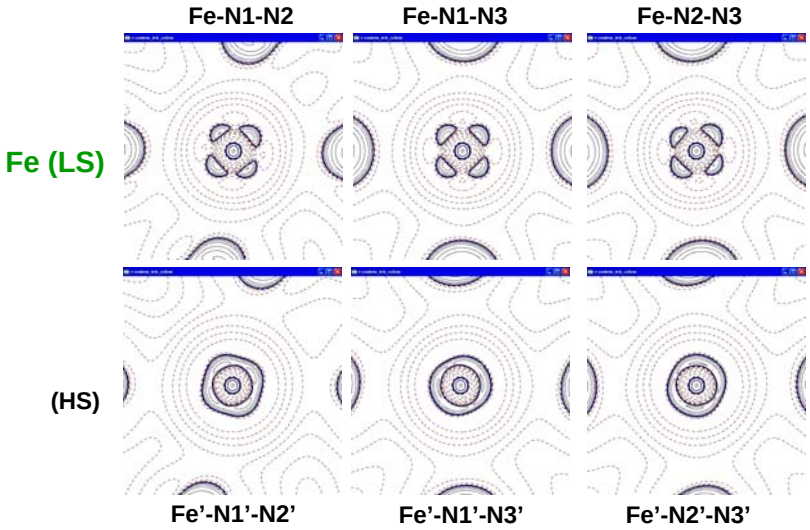

blue negative; red positive,

contours are $(-1)^l 2^m 10^n$ (l=1,0; m=1～3; n=-4～5) eÅ^{-5}.

70

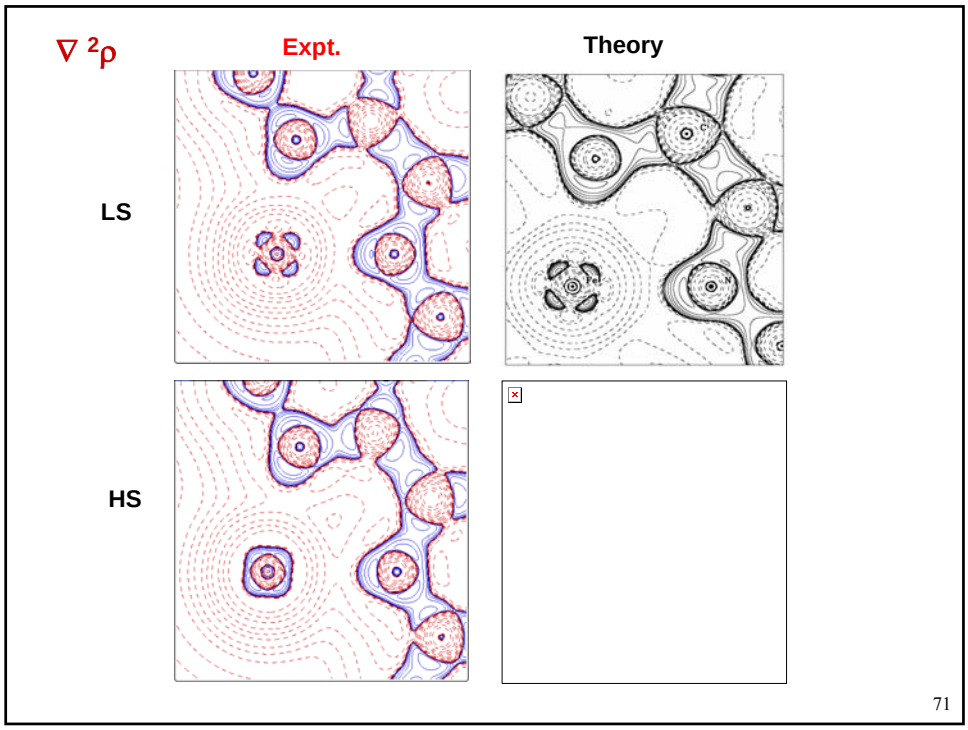
∇ 2ρ
Expt.
Theory
LS
HS
71

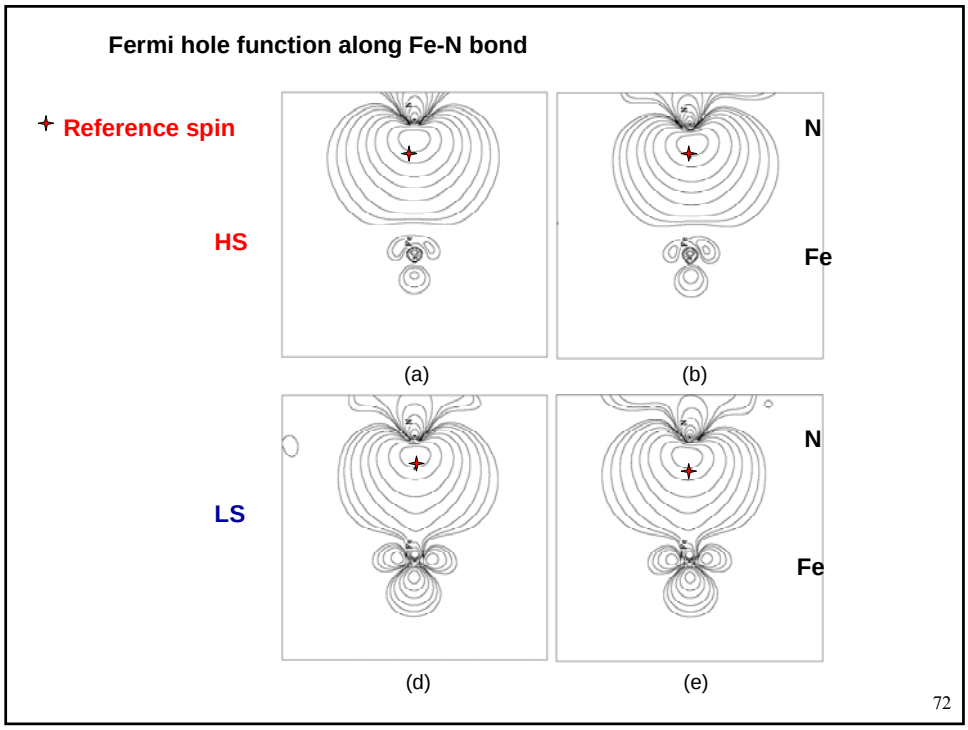
Fermi hole function along Fe-N bond
Reference spin
HS
LS
N
Fe
(a)
(b)
(d)
(e)
72

Iso-value surface of Laplacian around Fe

LS HS

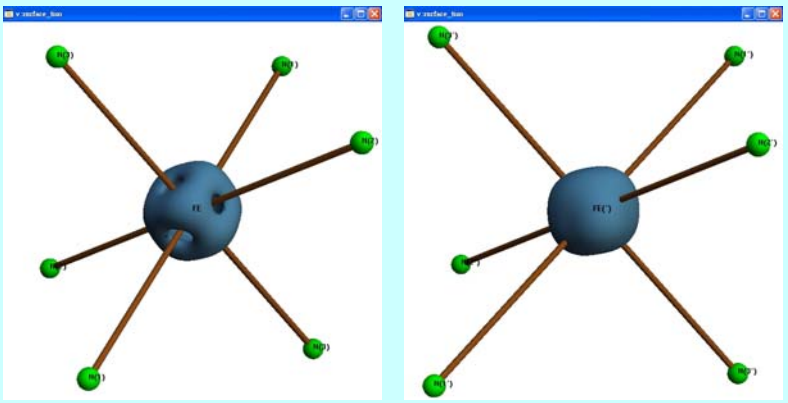

L=-100 eÅ^{-5}

73

d orbital populations of Fe

	$d_{z^2}(e_g)$	$d_{xy}(e_g)$	$d_{xz}(t_{2g})$	$d_{yz}(t_{2g})$	$d_{x^2-y^2}(t_{2g})$	total	
Fe (LS)	0.60	0.72	1.73	1.88	1.80	6.75	Expt
	0.40	0.37	1.76	1.88	1.93	6.34	DFT
Fe' (HS)	1.27	1.36	1.30	1.51	1.27	6.70	Expt
	1.09	1.06	1.03	1.05	1.86	6.09	DFT

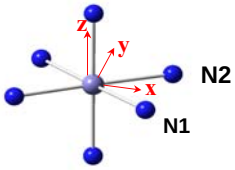

AIM charge and volume of Fe

		Fe(LS)	Fe'(HS)
Charge (e)	Expt.	1.05	1.18
	DFT	1.30	1.40
Volume (Å^3)	Expt.	7.79	9.79
	DFT	7.02	8.75

74

Hydrogen Bonds

Bond/ BP	O···O	ρ_c	$\nabla^2\rho_c$	G_b	H_b	Compound
O2···H6 1.219	2.432	1.190	-8.267	0.487	-1.066	$[H_2N(CH_3)_2][H(HC_4O_4)_2]$
O2···H1 1.226	2.451	1.434	-15.921	0.262	-1.376	$Mn(HC_4O_4)_2(H_2O)_4$
O3···H2 1.232	2.462	1.646	-25.050	0.020	-1.774	$Mn(HC_4O_4)_2(H_2O)_4$
O2···H3 1.794	2.744	0.340	1.898	0.222	-0.089	$Mn(HC_4O_4)_2(H_2O)_4$
O4···H6 1.757	2.696	0.393	1.683	0.248	-0.130	$Mn(HC_4O_4)_2(H_2O)_4$
O4···H3 2.764	3.183	0.054	0.701	0.039	0.010	$[H_2N(CH_3)_2][H(HC_4O_4)_2]$
S1···H1 2.880	3.506	0.08 0.10	0.53 0.90	0.04 0.06	0.00 0.01	S_7NH

75

Symmetrical hydrogen bonds

O2···H1···O2

ρ_c: 1.434

$Mn(HC_4O_4)_2(H_2O)_4$

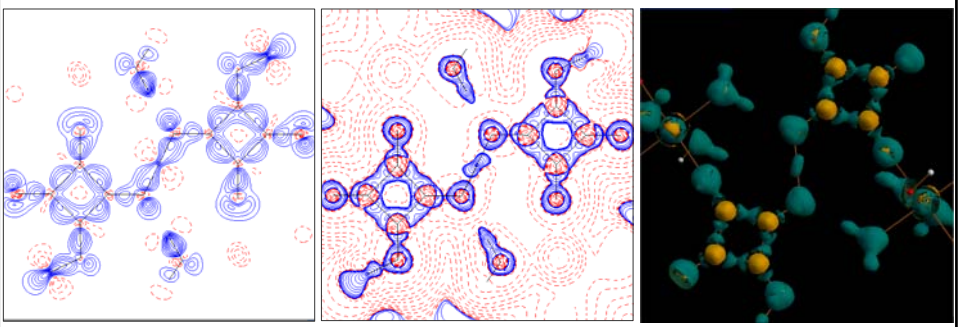

$\Delta\rho$ $\nabla^2\rho$ Iso-value surface of $\nabla^2\rho$

76

Symmetrical hydrogen bonds

O3···H2···O3

ρ_c: 1.646

$Mn(HC_4O_4)_2(H_2O)_4$

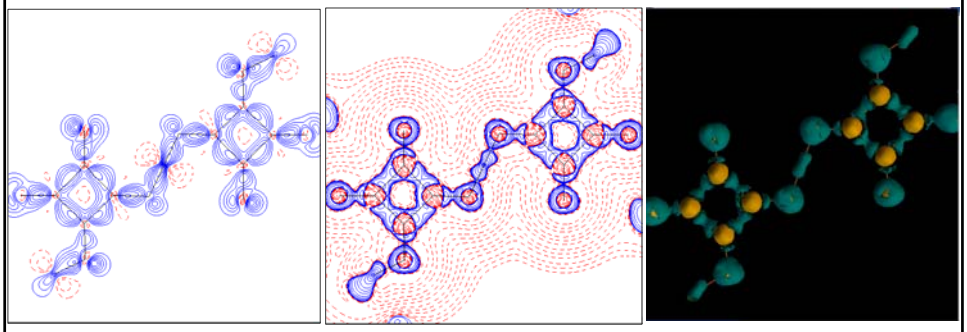

$\Delta\rho$ $\nabla^2\rho$ Iso-value surface of $\nabla^2\rho$

77

Iso-value surface of $\nabla^2\rho$

ρ_c: 0.486

O1···H5···O3

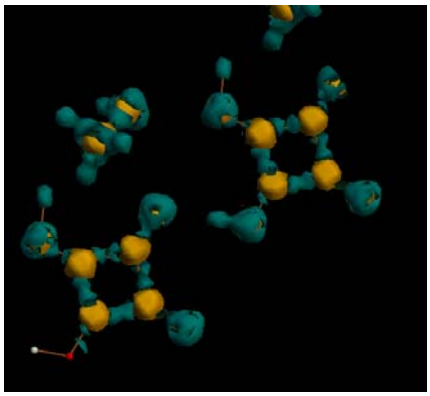

ρ_c: 1.190

O2···H6···O6

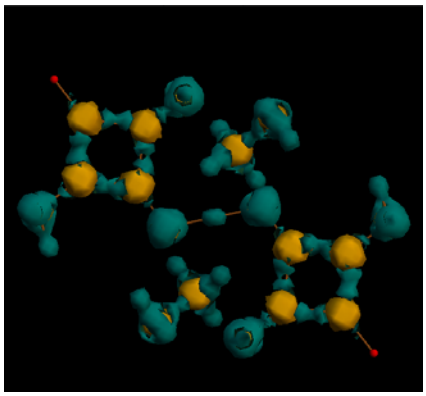

$[H_2N(CH_3)_2][H(HC_4O_4)_2]$

J. Phys. Chem., 1994, *Vol.98, No. 45*, 11685-11693

78

Inter-molecular Interaction

H-bond **C---S; N---O interaction**

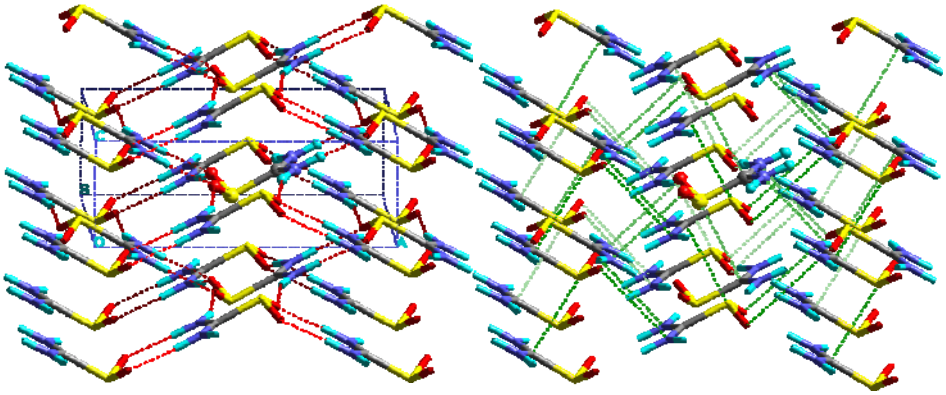

Thiourea-S,S-dioxide

Chem. Eur. J., 2003, *9*, 3112-3121

79

N-H1···O **2.837Å**
176.6
ρ_c: 0.178

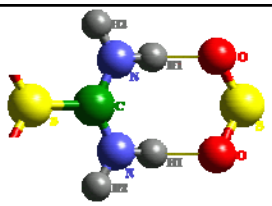

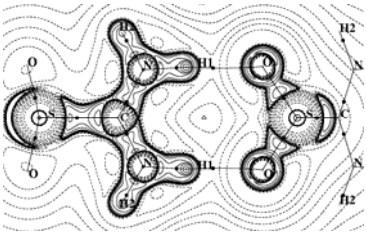

dimer(DFT)

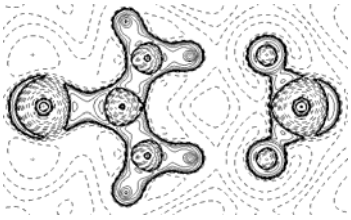

crystal(PDFT)

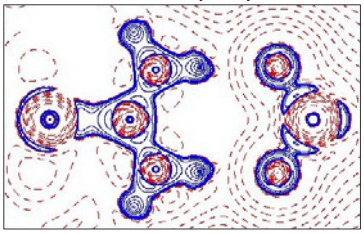

expt(XD)

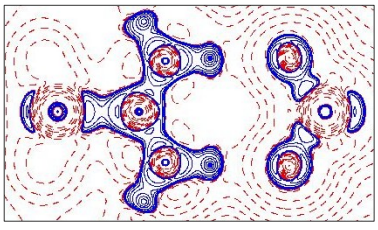

PDFT/XD

80

N-H2···O

2.826Å
158.4°

ρ_c: 0.146

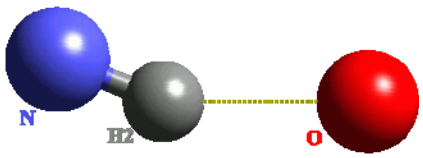

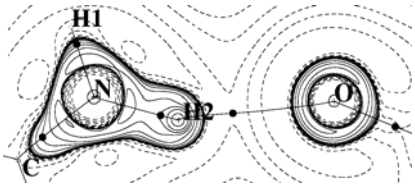

Dimer(DFT)

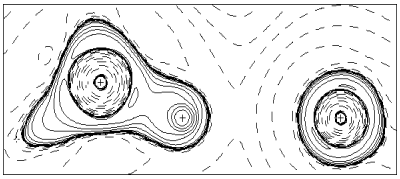

Crystal(PDFT)

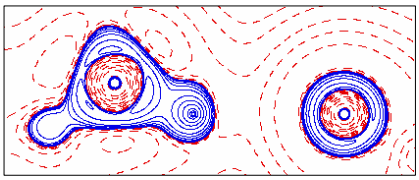

Expt(XD)

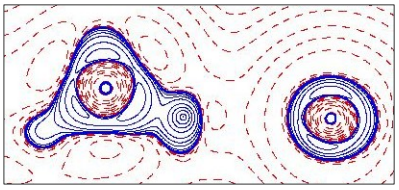

PDFT/XD

81

Weak intermolecular interactions
C ··· S' interaction

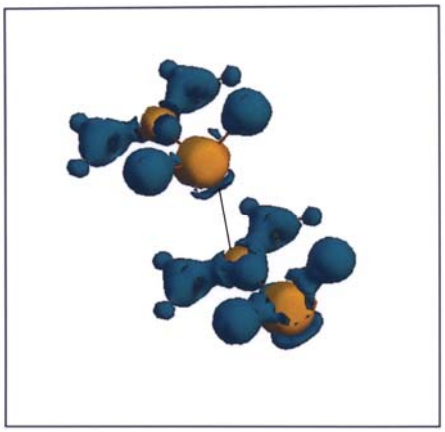

Expt

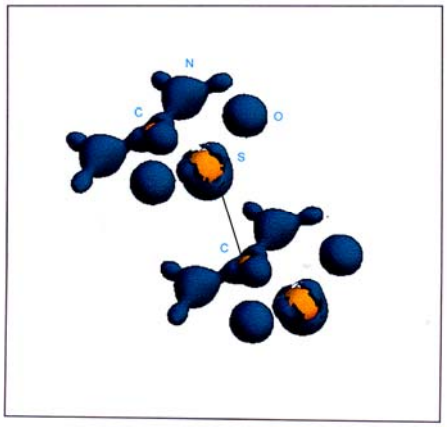

DFT

82

Net atomic AIM charge and molecular dipole moment (Debye)

Atom	Monomer	Heptamer	PDFT	PDFT/ XD	Expt/ KRMM
S	2.164	2.141	2.145	1.955	1.759
O	-1.313	-1.347	-1.362	-1.339	-1.255
N	-1.287	-1.386	-1.407	-1.246	-1.452
C	1.214	1.221	1.277	0.790	0.893
H1	0.410	0.502	0.522	0.611	0.671
H2	0.500	0.550	0.538	0.602	0.707
$-SO_2$	-0.46	-0.55	-0.58	-0.72	-0.75
$-C(NH_2)_2$	0.46	0.55	0.58	0.72	0.75
Dipole moment	12.6	14.2	14.6	15.5	16.3

83

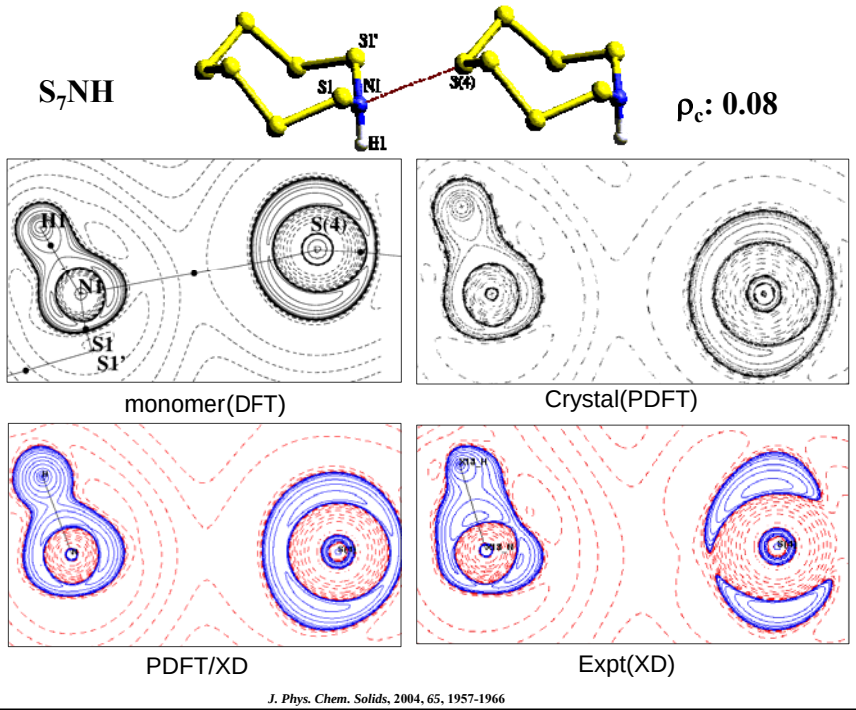

J. Phys. Chem. Solids, 2004, 65, 1957-1966

84

S_7NH

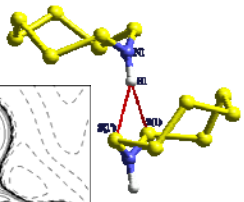

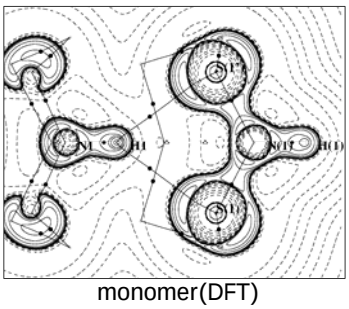

monomer(DFT)

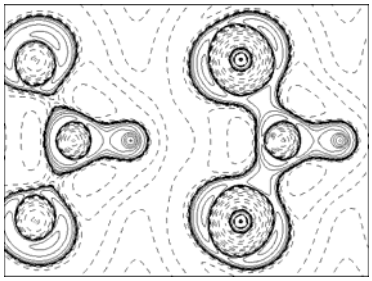

Crystal(PDFT)

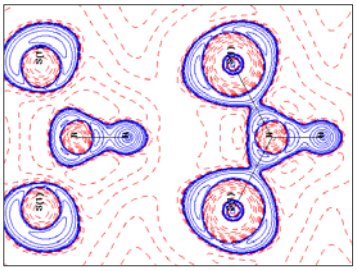

PDFT/XD

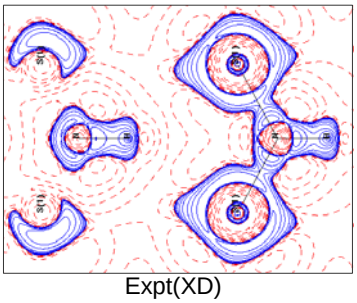

Expt(XD)

85

S_7NH

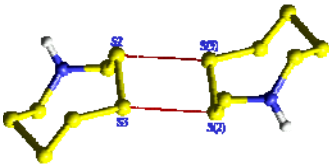

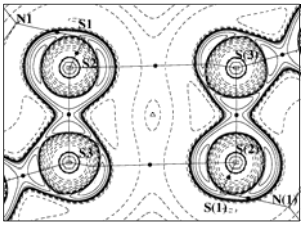

monomer(DFT)

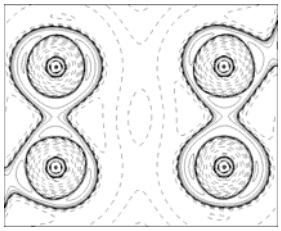

Crystal(PDFT)

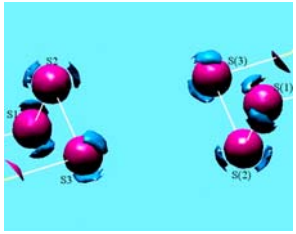

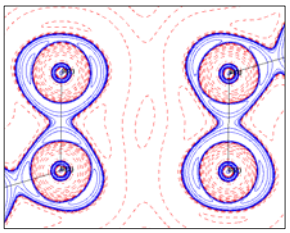

PDFT/XD

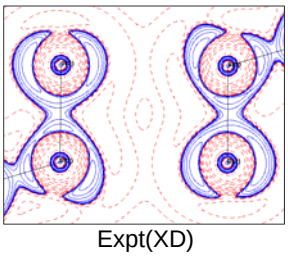

Expt(XD)

86

Secondary Interaction

Bond/BP	ρ_c	$\nabla^2\rho_c$	G_b	H_b	Compound
N···S4	0.07 0.06	0.64 0.61	0.04 0.04	0.01 0.00	S_7NH
S2···S3	0.06 0.05	0.36 0.61	0.03 0.04	0.01 0.01	S_7NH
S4···S3	0.06 0.04	0.67 0.53	0.04 0.03	0.01 0.01	S_7NH
S···C	0.06 0.05	0.77 0.65	0.04 0.03	0.01 0.01	Thiourea S,S-dioxide
O···N	0.02 0.02	0.26 0.27	0.01 0.02	0.005 0.004	Thiourea S,S-dioxide

87

Summary

- Accurate diffraction data in company with DFT calculations can be used as an effective tool for chemical bond characterization.
- Non spherical electron density can be visualized via deformation density maps.
- Bond characterization can be classified by the magnitude of $\rho(r_c)$, $H(r_c)$ and Fermi hole function.
- M-L coordinated bond is dative but with certain extent of covalency. Bond strength is such that M-N_{imine}> M-S > M-O.
- M-L multiple bond is covalent, the bond strength is much bigger than that of M-L coordinated bond.
- VSCC can be demonstrated by the isovalue surface of $\nabla^2\rho$, its quantitative description can be achieved by atomic graph.
- A range of H-bond is illustrated
  Weak intermolecular interactions are depicted.

88